Effect of Compressive Load on Oblique Pullout Capacity of Model Single Piles in Sand

A Thesis

Submitted in Partial Fulfillment of the Requirements

for the Degree of

MASTER OF TECHNOLOGY

By

Krishna B.

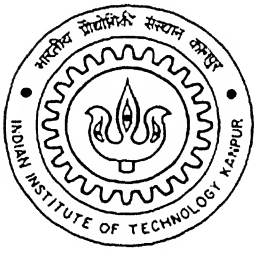

to the

Department of Civil Engineering

INDIAN INSTITUTE OF TECHNOLOGY KANPUR

JULY, 2004

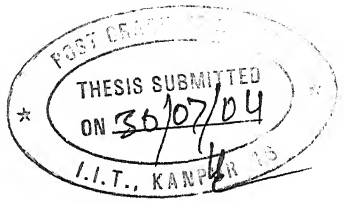

CERTIFICATE

This is to certify that the work contained in the thesis entitled "**Effect of Compressive Load on Oblique Pullout Capacity of Model Piles in Sand**" by Krishna B. has been carried out under my supervision and this work has not been submitted elsewhere for a degree.

Nihar Ranjan Patra 29/07/2004

(Dr. N. R. Patra)

Department of Civil Engineering,

Indian Institute of Technology,

Kanpur.

Abstract

An experimental program is conducted on model piles in sand to study the effect of compressive load (i.e. 0%, 25%, 50%, 75%, and 100% of their ultimate capacity in compression) on uplift capacity of piles under oblique pull. Model single steel piles of 20mmX20mm cross section, which had an embedded length of 400mm to 600mm, were installed in a tank of size 980mmX980mmX980mm. Uniformly graded "Ennore Sand" grade-II procured from Chennai (India), was used as a foundation medium. The pull was applied in 0^0, 30^0, 60^0 and 90^0 inclinations with vertical. The load-displacement response, variation of oblique resistance with % of compressive load, net oblique capacity, failure modes and variation of oblique capacity with L/d ratio has been studied. It has been observed that the net oblique capacity of piles decreases with increase in % of compressive load. Semi-empirical methods have been proposed based on experimental results to determine the oblique resistance of piles subjected to static compressive load. It takes to account the effect of angle of internal friction of the soil, angle of inclination of the pull, the ultimate uplift capacity and ultimate lateral resistance of pile. A comparison of predicted values of the ultimate oblique resistance by proposed methods of analysis with experimental values, and also with those reported by others, showed reasonably good agreement.

Key Words: Piles, Oblique loads, Compressive Loads, Sand

Acknowledgements

I take this opportunity to express my sincere gratitude toward my thesis supervisor Dr. N. R. Patra for his invaluable guidance. It would have never been possible for me to take this thesis to completion without his innovative ideas and his relentless support and encouragement. I consider myself extremely fortunate to have had a chance to work under his supervision. Learning how to do research and problem solving methodology from him has being a life time experiences in it self.

I also wish to thank whole heartily to Prof. N. S. V. Kameshwera Rao, Prof. M. R. Madhav, and Prof. Sarvesh Chandra for the invaluable knowledge they have imparted to me and for teaching the principles in most exciting and enjoyable way.

I would like to express my sincere thanks to Prof. P. K. Basudhar for his encouragement and friendly approach throughout my stay.

I also extend my thanks to A. K. Srivastava, Gulab chand, Kishan Pal Yadav, Parashuram and Verma for their excellent co-operation during the fabrication of experimental setup and during carrying out the experiments.

My stay at IITK was unforgettable to say the least, and the biggest reason for it being my classmates of the great mtech 2002 batch. I thank my classmates just for being such great buddies. My special thanks to Vanitha and Basha, Satyanarayana, Gautham, Sivaram, Srinu, Ravi, Dinesh, Bapi Raju, Prasad.

I would like to thank my parents for bringing me to this stage in life, it was their blessings which always gave me courage to face all challenges and made my path easier.

Krishna

CONTENTS

List of Figures

List of Photographs

List of Tables

Chapter I

Introduction

1.1 General

Pile foundations are generally used to transmit the superstructure loads to deeper strata when the subsurface soil is of inadequate strength. Extensive theoretical and experimental investigations have been carried out over the last few decades to study the behaviour of piles subjected to axial, inclined or lateral compressive loads.

Structures such as transmission towers, mooring system for ocean surface or submerged platforms, tall chimneys, jetty structures are subjected to uplift loads. The types of foundations to be adopted for these structures vary according to the suitability of the site conditions. When poor soil at shallow depth or problem of caving or water table arises, the geotechnical engineers are compelled to adopt deep foundation in the form of piles. Similarly, lateral forces act on, the foundations of quay and harbour structures due to the impact of ship during berthing and wave action, offshore structures subjected to wind and wave action, earth retaining structures and lock structures. Large inclined loads act on the foundations of retaining wall, anchors for bulk heads, bridge abutments, piers, anchorage for guyed structures and offshore structures which are generally supported on piles.

With the construction of superstructure, the compressive load on pile foundation gradually increases. The full compressive load comes on piles when the superstructure is completed. It is about 30-40% of the ultimate load carrying capacity of piles in compression. Generally the design of pile foundation under compressive loads is, in general, based on requirements that complete collapse of piles or the supporting structures should not occur even under the most adverse conditions and that the deflection at working loads should not be so excessive so as to impair proper functioning of the foundation. Thus, for structures, in which deflection may not be critical, the design is governed by the ultimate resistance of the piles with a suitable factor of safety.

Generally, ultimate capacity of piles under oblique pulling load depends on the embedded length, pile diameter, pile-soil friction angle, inclination of load, shear strength parameters and density of foundation medium. A good number of laboratory model and large-scale field test results on ultimate uplift capacity of single piles in granular soil are available (Downs and Chieurzzi 1966, Meyerhof and Adams (1968), Das and Seeley (1975), Awad and Ayoub (1976), Poulos and Davis (1980), Chaudhuri and Symons (1983), Levacher and Sieffert (1984), Chattopadhyay and Pise (1986), Alwayn et al (1999)). Similarly a good number of analytical solutions along with a large number of field and laboratory investigations are available to predict the load-deflection response and hence the ultimate resistance of laterally loaded pile (Broms (1964), Meyerhof and Ranjan (1972), Meyerhof (1973), Liu and Meyerhof (1987) and Prasad and Chari (1999)). Studies on the behaviour of piles under oblique pulling loads are limited (Yoshimi (1964), Broms (1965), Meyerhof (1973), Meyerhof and Ranjan (1973), Das, Seeley and Raghu (1976), Poulos and Davis (1980), Chattopadhyay and Pise (1986) and Ismael (1989)). A few have considered the effect of stage compressive loads on uplift capacity of single piles (Das and Pise(2003)). There is no quantitative and qualitative information available on the behaviour of piles under oblique pull when subjected to simultaneous compressive loads.

1.2 Need for Experimental and Analytical Study

From the review it is seen that systematic investigations on the quantitative and qualitative influence of the parameters such as length-to-diameter ratio, pile friction angle, inclination of load and effect of stage compressive loads (0%, 25%, 50%, 75%, 100% load of ultimate compressive load capacity of piles) on the behaviour of the piles under oblique pulling loads subjected to static compressive loads are not available. Field test results could yield the most rational approach for understanding the pile behaviour. However, the high cost measured both in time and money for obtaining high quality data from full-scale field tests and considering the large number of variables involved as described above led to determine if accurate data could be obtained by conducting model tests in the laboratory. In the absence of resources and scope of testing prototype, small-scale laboratory tests can substantiate the effects of above variables qualitatively and quantitatively on the behaviour of piles. Semi-empirical approaches based on the experimental observations would be helpful for predicting the

ultimate oblique resistance of piles under static compressive loads. These approaches should reflect the effects of the variables such as embedment length to diameter ratio, pile friction angle, soil density and obliquity of the load under simultaneous uplift cum compressive loads.

1.3 Scope of the Study

Laboratory Model tests have been carried out on model single steel piles of cross sectional area 20mmX20mm, embedment lengths of 400mm and 600mm embedded in dry sand under oblique pulling loads subjected to static compressive loads. Uniformly graded sand of standard grade-II procured from Chennai (India) is used as a foundation medium. The foundation bed is prepared in a model tank of size 980mmX980mmX980mm, with a uniform placement density of 1.58gr/cc (using Rain-fall Technique), angle of friction, $\phi=38^0$, soil-pile friction angle, $\delta=26.6^0$ and relative density of 54.3%. These piles were tested for different % of static compressive loads (0%, 25%, 50%, 75% and 100% of ultimate load in compression) at inclination of 0^0, 30^0, 60^0 and 90^0 with the vertical axis of the pile. The inclination lies in the vertical plane, which passes through the axis of the pile and is parallel to the length of the pile. The load-displacement response, variation of net oblique resistance with % of compressive load, failure modes and variation of oblique capacity with L/d ratio has been studied. Semi-empirical methods have been proposed based on experimental results to determine the oblique resistance of piles subjected to static compressive load. This study takes into account the effect of angle of internal friction of the soil, angle of inclination of the pull, the ultimate uplift capacity and ultimate lateral resistance of pile. A comparison of predicted values of the ultimate oblique resistance by proposed methods of analysis with experimental values, and also with those reported by others has been made.

Chapter II

Review of Literature

2.1 Introduction

During the past five decades a large number of investigations on the behaviour of pile foundations under different conditions of loading have been reported by many researchers. An attempt has been made in this chapter to review the available literature on analytical and experimental studies on ultimate resistance of piles in sandy soil under oblique pulling loads. The review here has been presented in chronological order under the following headings for convenience.

1) Axial uplift capacity of piles
2) Ultimate lateral resistance of piles
3) Ultimate resistance of piles under oblique pulling loads

2.2 Axial Uplift Capacity of Vertical Piles

Generally, the limiting frictional approach along with the equilibrium conditions is used to evaluate the uplift resistance of piles. The uplift capacity theories are based on the formation of the failure surface around the pile under the action of uplift load. The review is restricted to piles embedded mostly in cohesionless soils.

Sowa (1970) analyzed the field test results of cast-in-situ cylindrical pier. He found that k_s is considerably less than k_0 and k_a, where k_o is coefficient of earth pressure at rest and k_a is Rankine's active earth pressure coefficient. Analyzing the test results on concrete piles in sandy deposits reported by Adams and Hayes (1967), he concluded that very large value in excess of k_0 for k_s might occur.

Vesic (1970) considered the cavity expansion model. Based on the test results on a driven-instrumented pile in the predominantly sandy deposit he indicated that the ultimate skin friction on piles is same both in tension and compression. He concluded that beyond a critical value of 10d (d= diameter of a pile) in very loose sand and about

20d in very dense sand the average unit skin frictional resistance results into a fixed value which is a function of the relative density of sand and mode of placement of a pile.

Das, Seeley and Pfeifle (1977) conducted laboratory model test for ultimate uplift capacity of rough rigid piles in sand. Wooden piles 610 mm long and 25.4 mm in diameter, having embedment ratio L/d =24 were used. Angle of shearing resistance ϕ varied from 31^0 to 40.5^0 for loose to dense condition of sand. The corresponding δ/ϕ values were 0.4 to 1.0. It is concluded that unit skin friction during uplift at soil-pile interface increases linearly with depth up to a critical depth and it remains constant beyond it. The critical embedment ratio increases with relative density of compaction. A tentative procedure for estimating the gross uplift capacity has been proposed.

Ismael and Klym (1979) reported full-scale uplift test results on instrumented cylindrical pier, 1.07m in diameter and 6.4 m deep in compact fine to medium brown sand with some silt and trace of clay. The piers were installed by slurry displacement method. Analyzing the results, they suggested the use of same value in tension and compression of k_u as suggested by Adams (1975). These values varied from 0.5 to 2.0 for very loose to very dense condition of sand.

Poorooshasb and Parameswaran (1982) analyzed vertical uplift behaviour of a single rigid pile/pier embedded in frozen sandy soil. The stress-strain behaviour of soil is idealized to be linear. It is assumed that when a rigid cylindrical pile is subjected to vertical uplift forces, the deformation of the soil around the pile shaft can be idealized as shearing of concentric cylinders. The butt movement can be obtained in a closed form expression which is a function of pile radius, pile length, vertical load and elastic modulus of sand. Results of the analysis are represented by curves from which the butt movement can be estimated for given uplift forces. The analysis is applicable to relatively shallow piles embedded in moderately to heavily consolidated clays or to bore piles embedded in sensitive clays.

Levacher and Sieffert (1984) presented results of laboratory investigation on the influence of dynamical driving methods and relative density on behaviour of piles in

tension. The study includes 31 bored piles, 12 driven piles and 5 vibro-driving piles under pulling tests in dry sand. Steel model pile of 35mm outer diameter and 900 mm embedment depth was used in the testing program. Clean, poorly graded sand at a placement density 16.5 kN/m^3, angle of shearing resistance, ϕ =36^0 and moisture content of 4% was used as a foundation medium. The ultimate resistance was attained at displacement/diameter of 0.05-0.11 for bored piles, 0.07-0.14 for driven piles and 0.08-0.11 for vibro-driving piles. It is indicated that the average ratio of ultimate uplift resistance of driven pile to statically driven pile is 0.5 and that for vibro-driven pile is 0.67.

Subba Rao and Venkatesh (1985) presented laboratory studies on uplift behaviour of short piles in sands. Smooth and rough steel piles 12.7 mm in diameter, 320 mm in length and having L/d=10,15 and 20 were used in the investigation. Two types of uniform sand beds were used for testing. The frictional angle for dry sands was ranged from 36^0-40^0. The piles were tested under uplift as well as compressive loading. The uplift capacity was found to increase with L/d ratio, pile roughness, soil density and particle size. Pile movements of about 5% of the pile diameter in loose sand and about 10% of the pile diameter in dense sand were found to be necessary to mobilize the uplift capacity. These values were much more than 3% to 6% required for shaft loads during push-in tests. The unit skin friction during pull out tests was significantly less than in push-in tests.

Kulhawy (1985) presented a general analysis/design model for the drained uplift capacity of drilled shaft foundations. This model evolved from extensive research to define the failure mechanism and establish the controlling parameters. The uplift capacity of shaft was given by

$$Q_u = W + Q_{tu} + Q_{su}$$
$$= W + Q_{tu} + \int_{surface} \tau\,(z)\,dz \qquad (2.1)$$

Where, Q_u= uplift capacity

W= foundation weight

Q_{tu}= tip resistance

Q_{su}= side resistance

τ = shearing resistance along a general shear surface

The author reported that the shaft had failed principally along the soil shaft interface leading to an overall cylindrical shear. The corresponding load transfer increased from Q_{tu} at tip to Q_u at top. Considering all the factors governing side resistance viz. angle of wall friction, operative coefficient of horizontal stress etc, the following equation could be established.

$$Q_{su}= K/K_o=\int_o^D p(z)\, \sigma'_v(z)\, K_o(Z) \tan[\, \phi'(z)\, \delta'/\phi'\,]\, dz \text{ ----------(2.2)}$$

Where, p= foundation perimeter

σ'_v= vertical effective stress

k = operative coefficient of horizontal stress

ϕ'= effective angle of shearing resistance

δ'= effective friction angle for soil shaft interface with $\delta'/\phi'=1$ and $k/k_o=2/3$ to 1 (for concrete)

Ismael and Aïsanad (1986) examined the uplift capacity of bored piles in dense calcarious soil by field tests at three sites in Kuwait. The nine test piles were 0.5m diameter and extended to a maximum depth of 15m below the ground surface. The mobilized skin friction and the coefficient of lateral earth pressure were determined and compared with the values obtained in non-calcarious sand. Test results were compared with empirical co-relations relating skin friction to the standard penetration test results. They concluded that bored piles developed substantial skin friction in dense weakly cemented calcarious sandy soils. The skin friction increased with depth for shallow depth range. The coefficient of lateral earth pressure in uplift varied between 1 and 1.2. For the piles, where failure reached, the average value of the coefficient was 1.05. Failure of bored tension pile was usually reached at an upward deflection of 5 to 10 % of pile diameter. The higher value was associated with relatively deeper piles.

Chattopadhyay and Pise (1986) proposed an analytical method to predict the ultimate uplift capacity of piles embedded in sand, based on the assumed failure surface. In the derivation of uplift capacity of vertical pile in sand, they considered the angle of shearing resistance (ϕ) of the soil, the pile friction angle (δ) and L/d ratio. During uplift of a pile, an axi-symmetric solid body of revolution of soil along with pile is assumed to move up along the resulting surface. The movement is resisted by the mobilized shear strength of the soil and pile. In the limiting equilibrium condition, ultimate capacity of pile is attained. In proposing the theory they assumed the failure surface to be curved starting tangentially to the pile surface and reaching the ground surface (at $(45^0-\phi/2)$). They proceeded with the assumed slope of failure surface at any height 'z' above the pile tip as

$$dz/dx = \tan(45^0-\phi/2)\, L/z\, \exp.\beta(1-z/L) \quad \text{----------(2.3)}$$

where, $\beta = \lambda(50-\phi)/2\delta$.

L= embedment depth

ϕ = angle of shearing resistance of soil

δ = angle of wall friction

λ= slenderness ratio

The expression, $\beta = \lambda(50-\phi)/2\delta$, has been arrived at on the assumption that the maximum value of ϕ for practical purposes will be 50^0. Integrating with proper boundary conditions and simplifying, the extent of failure surface is arrived.

It is assumed that in the limiting equilibrium condition, ultimate capacity of pile is attained when the mobilized shear strength along the failure surface and the weights of the body of the soil and pile balance the applied forces. They have derived the expression for the net uplift capacity of the pile P_{un},

$$P_{un} = A_1\, \gamma\, \pi\, d\, L^2 \quad \text{----------} \quad (2.4)$$

Where, P_{un} = net ultimate uplift capacity

γ = unit weight. of soil

Average skin friction, P_{av}, in dimensionless form is

$$P_{av}/\gamma\, d = A_1\, \lambda \text{ ---------- (2.5)}$$

Net uplift capacity factors are given elsewhere (Chapter-V, Figure 5.2) for convenience. They depend on angle of shearing resistance of soil,ϕ, pile friction angle,δ, and embedment length to diameter ratio.

Turner and Kulhawy (1990) carried-out experimental study on the effect of repeated loading on drained uplift capacity of drilled shafts in granular soil. The mechanism causing changes in drilled shaft resistance was identified and the effects of initial soil density, shaft depth to diameter ratio and the magnitude of repeated loading were evaluated. Critical levels of loading were established above which the shaft failed in uplift and below which failure did not occur. Implications for the design of drilled shafts under repeated axial loading were presented.

Alawneh, Malkawi and Al-Deeky (1999) conducted sixty-four pullout tests on open and close-ended rough and smooth model piles of 41 and 61 mm diameter. The model piles were installed in medium dense and dense sand to an embedded depth of 0.8m by static jacking and driving. The values of ϕ and γ were 39^0 and 48^0 and 15.2 kN/m^3 and 16.4 kN/m^3 depending on the compaction of sand. The results indicated that pile placement method, initial sand condition, pile surface roughness and pile end type were significant variables affecting the ultimate uplift shaft resistance of a single pile. Average unit shaft resistance of the driven model pile was 1.33 times that of the jacked model pile in dense condition and 1.52 times in medium dense sand condition. Rough piles experienced a 12-54 % increase in capacity compared with smooth model piles. The lateral earth pressure coefficient for rough model pile was greater than that for smooth pile. They attributed the increase in capacity of rough piles due to pile surface roughness, which increases the radial effective stress during tensile loading.

2.3 Ultimate Lateral Resistance of Vertical Piles

The behaviour of laterally loaded piles has been generally analyzed using the concept of sub-grade modulus or elastic continuum approach. A large number of analytical solutions and laboratory investigations are available on load-displacement response of single piles are summarized by Poulos and Davis (1980). Some attempts for the exact solution of flexible piles in elasto-plastic soil mass have been made by (Randolph (1977), Rowe and Poulos (1979), Kuhlemeyer (1979). The review here has been restricted to the ultimate resistance of laterally loaded piles in sandy soil.

Theoretical attempts have been made to evaluate the ultimate lateral resistance of laterally loaded single piles by categorizing the piles into short or rigid piles and long or flexible piles. Failure of the short pile under lateral loading is assumed to take place when the lateral earth pressure reaches the ultimate value along the length of pile. Long pile is assumed to fail where maximum bending moment induced in the pile attains the yield moment of resistance of the pile section. Further, in individual cases, it is mobilized depending on the end condition of the pile.

Broms (1964) on the basis of measured maximum earth pressure (Prakash (1962)) assumed that full passive earth resistance equal to three times the Rankine's passive earth pressure develops close to the location of the center of rotation for short piles. In case of long free head pile ultimate lateral resistance can be determined by the yield moment of resistance of pile section. In such cases, maximum moment occurring at the point on the pile where zero shear occurs shall be calculated assuming full mobilization of soil resistance above the point. He assumed that at the point of hinge, the passive earth pressure developed is equal to three times Rankine's passive earth pressure. Since no rigid demarcation between long or short free head pile exists, ultimate lateral resistance of a pile shall be taken as the lesser of (1) ultimate resistance required to cause failure of soil along the length of pile and (2) lateral load required to produce maximum bending moment equal to the yield moment of resistance of the pile section (Poulos and Davis, 1980).

Meyerhof and Ranjan (1972) presented an analysis to evaluate the earth pressure distribution on short vertical rigid pile subjected to horizontal load. In the state of

failure the pile fails by rotation about a point on the pile axis as a rigid body. The resulting passive earth pressure generated on the face of the pile is given by

$$p_z = \gamma\, z\, k_p^{\,z} \text{ ----------(2.6)}$$

where,

p_z= horizontal earth pressure per unit front area of the pile at a depth z below ground surface.

$k_P^{\,z}$= coefficient of earth pressure which depends on L/d ratio, angle of shearing resistance ϕ, of soil and pile friction angle δ.

Values of $k_P^{\,z}$ for different ϕ and δ combinations have been presented by Ranjan and Bhargava (1974). The ultimate resistance may be evaluated by static approach.

Meyerhof (1973) presented a semi-empirical expression to calculate the ultimate lateral resistance (P_L) of the vertical rigid rough piles by introducing horizontal uplift coefficient k_b' and it may be expressed as

$$P_L = \gamma\, L^2\, k_b'\, d/2 \text{ ----------(2.7)}$$

The horizontal uplift coefficient k_b' depends on L/d ratio as well as angle of shearing resistance ϕ of the soil. The values of k_b' for different angle of shearing resistance ϕ have been given by Meyerhof (1973) graphically.

Liu and Meyerhof (1987) carried out non-linear analysis of laterally loaded flexible piles and have shown that L_{eff}/L (the ratio of effective depth to the actual depth of embedment) depends not only on the pile stiffness K_{rs} but also L/d (length to diameter ratio) and other factors. The average relationship between L_{eff}/L and K_{rs} of the free head pile is approximately given by

$$L_{eff}/L = 1.8\ (K_{rs})^{0.12} \leq 1 \text{ ----------(2.8)}$$

Prasad and Chari (1999) measured the actual soil pressure distribution in model pile, embedded in sand, along its length across the diameter. A smooth steel pipe with an outside diameter of 102mm, length of 1135 mm and wall thickness of 5.6mm was used as instrumented pile. The tests were conducted in well-graded angular dry sand at loose density γ =16.5 kN/m^3 and ϕ= 33.3^0, medium density, γ =17.3 kN/m^3 and ϕ= 39^0 and dense state γ =18.3 kN/m^3 and ϕ= 43^0. Based on the experimental observations a method is suggested to predict the soil pressure distribution and the ultimate capacity of rigid piles. They found that the predictions are in closer agreement with the various field and laboratory observed results.

2.4 Ultimate Resistance of Piles under Oblique Pulling Loads

Extensive theoretical and experimental investigations have been carried out to study the behaviour of piles subjected to axial and inclined loads. However, investigations are limited under oblique pulling loads. The review has been made here on piles subjected to both inclined and pulling loads to understand the effects of parameters such as size, shape, embedment length, angle of inclination, pile friction angle, and placement density on the behaviour of piles.

Yoshimi (1964) studied the load-displacement response of piles under oblique pulling loads for rigid piles. The analysis has been extended by Ramnathan and Aiyar (1970) for flexible piles.

Broms (1965) analysed the test data of Yoshimi (1964) to predict the ultimate resistance of rigid piles. He assumed that the vertical component of the applied load does not affect the ultimate lateral resistance of the piles, while the normal component increases the axial uplift capacity of the pile. To evaluate the modified capacity, he assumed a passive pressure coefficient equal to five times the Rankine earth pressure coefficient and also replaced the negative pressure below the point of rotation by a force at the tip of the pile.

Meyerhof (1973) indicated that the net ultimate resistance P_θ, of a pile is a continuous function of the inclination θ of the pull. A semi-empirical expression to evaluate it for a rigid rough pile embedded in sand has been given as

$$P_\theta = (\gamma L^2 k_b'/2)\ d \text{ ----------(2.9)}$$

Where k_b' = uplift coefficient of a circular vertical pile for inclination of load θ

The values of k_b' for vertical and horizontal pull have been presented through figures for different values of ϕ for sandy soils. For an intermediate value of θ linear interpolation is suggested.

Meyerhof and Ranjan (1973) conducted model tests on two pile bents with embedment ratio of 13 and 23 for free standing bents and 15 and 25 for pile bents to estimate the ultimate capacity under inclined compressive load in compact and dense sand. Bents with vertical and batter piles have been tested under inclination of the load varying from vertical to the horizontal. The spacing of piles in the bent was kept at three times the pile diameter. They suggested that the ultimate capacity of a free standing pile bent under inclined load could be estimated by including horizontal soil resistance provided by the front face of the equivalent block footing and uplift resistance of rear piles. The ultimate load for a piled bent is higher than a corresponding free standing bent due to the load carrying capacity of the pile cap.

Das, Seeley and Raghu (1976) investigated model test results for the resistance of rigid rough vertical piles subjected to oblique uplift load in loose sand. Wooden piles of diameter 25mm were used as model piles. The embedment lengths to diameter ratios were 12 and 8. The angle of friction, ϕ, at the average density of the test was 31^0. Sudden failure was observed when the inclination of the applied load with respect to the vertical was less than about 30^0. Large displacement for a small increment of applied load has occurred for θ greater than 30^0. The prediction of the uplift capacity under oblique pulling load was done by the use of the approximate interaction relationship suggested by Meyerhof (1973). The predicted values are found to be fairly good with the experimental observations.

Poulos and Davis (1980) proposed a simplified method to predict the net ultimate resistance of vertical pile under oblique pulling loads. Depending on the net ultimate

uplift capacity, P_u, and ultimate lateral capacity, P_L, of the pile, the net ultimate resistance, P_θ, of the pile under a load at an angle θ to the vertical is assumed to be the lesser of the two values (i) $P_u \sec\theta$ and (ii) $P_L \operatorname{cosec}\theta$.

Chattopadhyay and Pise (1986) proposed a semi-empirical theoretical expression based on the experimental results to evaluate the ultimate resistance of pile embedded in sand under oblique pulling loads. They have taken into account the effects of angle of inclination of the pull, ultimate vertical uplift capacity (P_u) and ultimate lateral resistance (P_L) of the pile. Model tests were conducted on smooth, medium rough and rough model piles in dry sand of density 1.60 g/cc corresponding to the angle of shearing resistance 41^0. For each type of pile three embedment lengths of 24.6, 49.6 and 74.4 cm were used. The pile friction angles for smooth, medium rough and rough piles were 15^0, 34^0 and 37^0. Pulling tests were carried out at an inclination of $\theta = 0^0$, 30^0, 60^0 and 90^0 to the vertical axis of the piles. The ultimate resistance, P_θ, of the pile was evaluated in polar diagrams in dimensionless terms P_θ/P_u versus θ for $\alpha = P_u/P_L < 1$ and $\alpha = P_u/P_L > 1$. It is found that the net ultimate resistance of a pile to the oblique pull is a continuous function of the angle of inclination of the pull and the ratio of net axial vertical uplift capacity and ultimate lateral resistance of the pile. For $\alpha > 1$, the maximum resistance to oblique pull is attained at $\theta = 30^0$. For α between 0.18- 0.72, it is attained at $\theta = 60^0$ and for $\alpha < 0.18$, the maximum resistance is mobilized at $\theta = 90^0$. Reasonable agreement is noted between the predicted and the observed values.

Ismael (1989) conducted field tests on bored piles subjected to axial and oblique pull in fine medium dense sand. Tests were carried out under axial uplift loading, lateral loading and oblique loading at an angle of 30^0 with the pile axis. The piles were 101 mm in diameter and 1.5m long. It is concluded that either the lateral resistance or axial capacity of the pile controls the pull out capacity under oblique loads, whichever is small. Failure under oblique pull was caused by lateral failure as lateral component of the load under oblique pull is close to the failure load from lateral load tests. However, the vertical component under oblique pull is well below the failure load determined from the uplift tests. The failure load under oblique loading was only 74% of the corresponding value under axial pull. They defined the critical angle as the angle of inclination between the applied tension load and the pile axis at which failure changes

from axial failure to lateral failure. Critical angle depends on soil properties, pile type and geometry.

Dash and Pise (2003) conducted laboratory tests on model tubular steel piles. The model piles were of 25mm outside diameter, 2mm wall thickness and embedment length /diameter ratio's of 8, 16 and 24. The piles were embedded in sand having soil-pile friction angles were 21 and 29 in loose and dense conditions of sand. The piles were subjected to static compressive loads of 0, 25, 50, 75 and 100% of their ultimate capacity in compression and subjected to pull out tests. The results indicated that the compressive load effect decreases the net uplift capacity of piles. A logical approach had been suggested to evaluate the net uplift capacity of piles under compressive load based on experimental results.

2.5 Conclusions

From the above review of literature, it has been found that a good amount of work has been done on single pile both theoretical and experimental. However, investigations on the behavior of piles under oblique pulling loads subjected to static compressive load are practically not available.

There are several variables such as shape, length to diameter ratio, soil type and placement density of soil and pile friction angle which affect the behaviour of pile under oblique pulling loads. A generalized semi-empirical approach validated with the test results considering all these parameters is needed to investigate the resistance of piles under pulling loads. Therefore, the present experimental and analytical investigations have been taken up.

Chapter III

Experimental Setup and Testing Programme

3.1 General

The aim of this investigation was to find out effect of % of static compressive loads on oblique pull out capacity of piles embedded in sand. This included the study of the behavioral aspects of the piles in terms of various parameters involved.

Model study is one off the means of fulfilling the objective as mentioned in the beginning. The added advantage of the model study is that the pertinent parameters influencing the behavior of piles can be controlled easily as per requirement, in addition the cost of carrying out model investigation is very much less and is much more convenient compared to field tests. Model study was therefore adopted in the present investigation in view of the advantages mentioned above; the relevant parameters considered for the study are

(a) Length of embedment
(b) Compressive loads
(c) Oblique pulling load.

In this chapter an attempt has been made to present the experimental set up, testing procedures.

3.2 Experimental Setup

The complete experimental setup is shown in Plate No.3.1 and Figure 3.1. The test setup consists of the following parameters.

a). Model tank
b). Foundation Medium
c). Device for pouring sand.
d). Arrangement of application of oblique pulling load.
e). Measuring devices (Dial gauges).

a) Model Tank

Tests were conducted in a fabricated metallic tank of size 980mmx980mmx980mm deep shown in Figure 3.1 and Plate No 3. 1

b) Foundation Medium

Uniformly graded "Ennore Sand" grade II obtained from Chennai (India), was used as a foundation medium. Selection of sand as foundation made because its behavior is free from time effects and reproducible densities can be achieved reasonably well. The specific gravity and uniformity coefficient of the Ennore sand were 2.65 and 1.71 respectively. Grain size distribution curve is shown in Figure 3.4. The sand grains are sub angular and limiting void ratios were, e_{min} = 0.5774, e_{max} = 0.7958 corresponding to maximum and minimum dry densities 1.68 gm/cc and 1.47 gm/cc respectively. The placement density was 1.58gm/cc, medium dense packing R.D 54.3%. The angle of shearing resistance for medium dense packing was 38^0 and soil-pile friction angle was 26.6^0.

c) Sand Pouring Device

Slot hopper having 5mm slot at one edge was used for pouring the sand by rainfall technique in the tank. Figure 3.4(a), 3.4(b) and Plate No 3.2 show the sand pouring device.

d) Loading Arrangement

Compressive loads are directly applied to pile cap centre. Pulling loads were applied in various inclinations (i.e vertically, obliquely and horizontally) at the pile cap through a double pulley (frictionless) arrangement. Flexible steel wire rope attached to the nut and bolt at the top of the pile cap. Wire rope was taken first through the adjustable pulley near the pile head then over a second pulley to the loading pan where dead weights were put for loading.

e) Measuring devices

For measuring axial (Vertical), lateral (normal) displacement and pile cap rotation, sensitive magnetic base dial gauges were used. Two dial gauges of travel 5cm were used for measurement of vertical displacement and two dial gauges of travel 2.5cm were used for measurement of lateral displacement of pile head. The sensitivity of dial gauge is 0.01mm as shown in plate No. 3.3.

3.3 Testing Programme

Various parameters

1. Embedment Length, L = 400mm; L/d=20
   = 600mm; L/d=30
2. Pile Dimensions = 20x20mm square.
3. Stages of compressive load = 0%, 25%, 50%, 75% and 100% of ultimate compressive load of respective piles.
4. Relative density for medium Dense packing (R.D) = 54.3%
5. Angle of Inclination with the pile axis (vertical) = 0^0, 30^0,60^0, 90^0

The detailed experimental program considering the above parameters is shown in Table 3.1.

3.4 Experimental Procedure

The experimental testing procedures for all piles (L/d =20 and L/d =30) are similar. It is described below.

3.4.1 Placement of Piles

Piles were placed in the empty tank suspended vertically resting on mild steel thin narrow plates placed over the edges of the tank

3.4.2 Pouring of sand and Tank Filling

The technique of sand placement plays an important role in the process of achieving reproducible density. After proper placement of the piles in empty tank, sand was poured in the tank continuously through the slot of the hopper keeping height of fall about 30cm for medium dense packing, moving horizontally by hand. This technique of sand pouring is termed as rainfall technique and this technique was

reported to achieve good reproducible densities (Patra (2001)). After half or more of the pile length was embedded in sand, pile caps were carefully removed. Further sand poring was continued till the required embedment depth was reached. The sand surface was leveled carefully. This method of sand pouring gave a predetermined dry density of 1.58gm/cc for medium dense sand (shown in plate No. 3.4).

3.4.3 Testing Procedure

The schematic diagram of the experimental setup (shown in Figure 3.1) shows the uplift test under the presence of static compressive load subjected to oblique pull. The following tests are carried out for a given L/d ratio of a pile in a given medium density of sand.

- Compression test
- Tension test (without any compressive loading subjected to oblique pull)
- Simultaneous compression and tension tests (with different static compressive load and oblique pull)

Compression Test

This test is meant for the assessment of the ultimate load carrying capacity of pile in compression. This test is conducted for embedment length of 400mm and 600mm. In each test the pile was suspended centrally in an empty tank by using the mild steel flat plates and C-clamps. Sand was poured by the rainfall method to attain the required embedment length. The compressive load was applied manually placing the loads on the surface of the pile cap. The corresponding deflection was recorded from dial gauges, placed at equidistance from the center of pile. From the set of load displacement curves the ultimate load carrying capacity in compression was determined.

Tension Test

These tests were meant for the assessment of the ultimate uplift capacity of piles without any compressive load (i.e. 0 % compressive load) acting on the piles. The placement of pile and pouring of the sand was carried out in identical manner as in a compression test. The pulling load was applied manually by means of an inextensible wire rope passing over a friction less pulley. In the case of oblique pull (i.e. 30^0, 60^0 and

90^0 with vertical) the vertical deflection was measured by two dial gauges placed vertically at 180^0 apart and two more dial gauges are provided horizontally to measure lateral deflection. The load displacement curves were plotted for different piles. From these the gross ultimate uplift capacity of the piles was determined. The net uplift capacity was worked out by subtracting the weight of the pile and other accessories from the gross ultimate uplift capacity.

Simultaneous Compression and Tension Test

These tests were carried out for the assessment of the effects of compressive load on pull out behavior of the piles under oblique pull. The arrangement made is similar to that of tension test except placing a static compressive load on pile cap. Then, the uplift load was applied in increments by means of inextensible wire rope. From the load displacement response the ultimate uplift capacity of pile was determined and hence the net uplift capacity was worked out by subtracting the weight of the pile, static compressive load and other accessories from the gross ultimate uplift capacity.

3.4.4 Load Application and Observation

The flexible wire rope passing over the pulleys was connected to the center of pile cap by means of specially fabricated U-hooks and the other end was attached to the loading pan. The position of the first pulley (i.e. adjustable one over the tank fitted to the channel section with nut-bolt) was fixed according to the position of the pile. Two flat mild steel plates were placed across the tank and magnetic base dial gauges were fitted to these flat plates by using c-clamps. These two dial gauges were placed at equidistance from the center of the pile cap. Two removable L-shaped stiff aluminum plates were fitted at the top of pile cap as shown in Plate No. 3.3. Axial displacements were recorded by dial gauges placed vertically and lateral displacement was measured by horizontally placed dial gauges. The rotation of the pile cap has been calculated using the axial displacement and half the distance between the two dial gauges measuring axial displacement. Then compressive load is placed on the center of the pile cap and left for some time so that the dial gauge readings remain stable. Then the uplift loads were applied by dead weights over the loading pan starting from the smallest with gradual increases in stages. Dial gauge readings were recorded when they were stable.

3.4.5 Verification of Sand Density

Density of sand in the tank was checked at the end of each test by a dynamic penetrometer. Figure 3.4(c) shows the sketch of the penetrometer. It consists of 9.5mm diameter mild steel rod with a conical tip at the bottom, and is provided with an arrangement such that a 2.49kg annular weight falls freely through a height of 30cm, on a platform fixed to the rod. Depth of penetration was recorded for 1, 2, 3, 4, 5, 6 and 7 numbers of blows. The depth of penetration recorded at different locations in the tank were practically same in all the tests for equal number of blows indicating uniformity of density during different sand filling. Typical values of penetration depth for number of blows 1, 2, 3, 4, 5, 6 and 7 were 20cm, 28cm, 35cm, 42cm, 49cm, 55cm and 60cm respectively for medium dense packing.

Table 3.1 Experimental programme

Medium Dense Sand				
L/d Ratio	**Compression Tests**	**Tension tests**		**Total No of Experiments**
		Angle	**%of compressive load**	
L/d = 20	1	$\theta = 0^0$	0	20
		$\theta = 30^0$	25	
		$\theta = 60^0$	50	
		$\theta = 90^0$	75	
			100	
L/d =30	1	$\theta = 0^0$	0	20
		$\theta = 30^0$	25	
		$\theta = 60^0$	50	
		$\theta = 90^0$	75	
			100	
Total = 1+1+20+20 = 42				

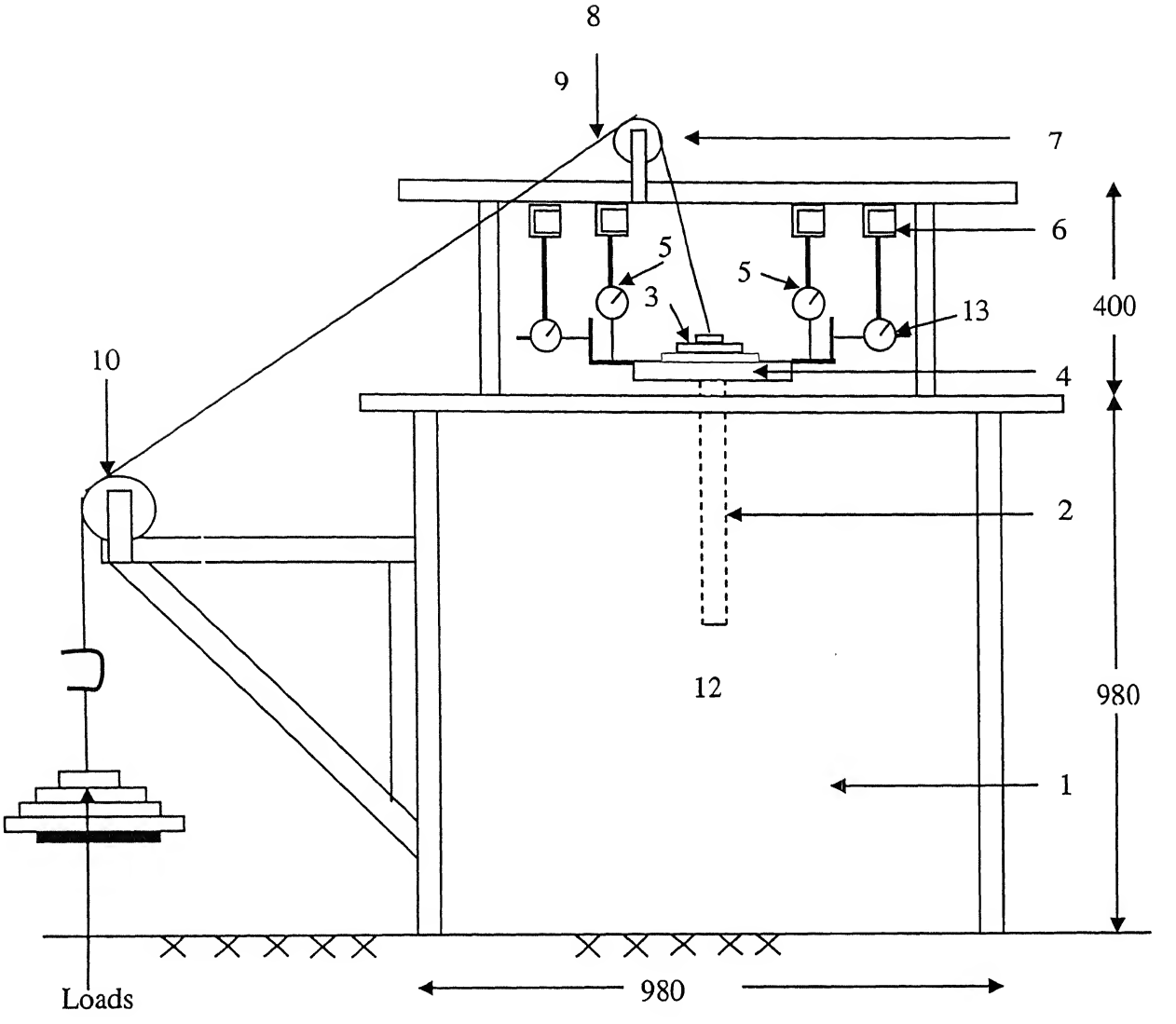

Figure 3.1 Experimental setup

1. Model Tank
2. Piles
3. Static compressive load
4. Pile cap
5. Vertical dial gauge
6. Magnetic base plate
7. Pulley 1
8. Wire rope
9. Aluminium Strip
10. Pulley 2
11. Loads
12. Sand Deposit
13. Horizontal dial gauges

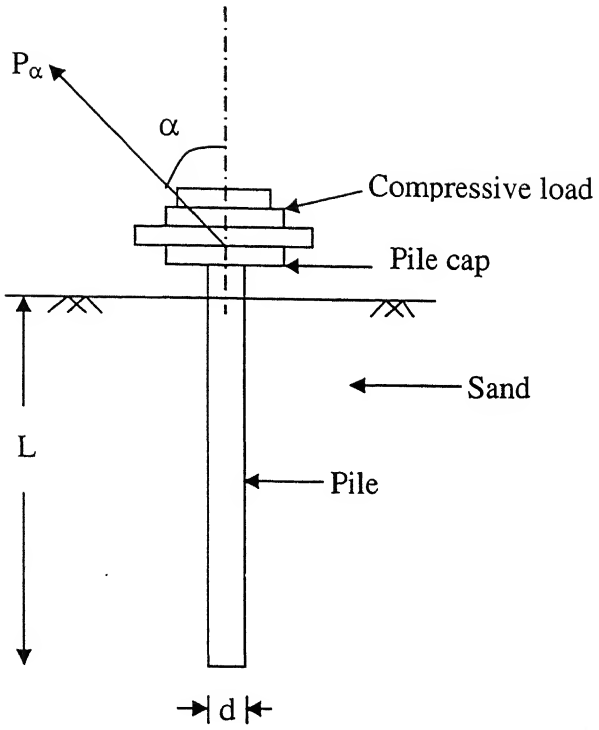

Figure 3.2 Line diagram of piles under oblique pull subjected to compressive load

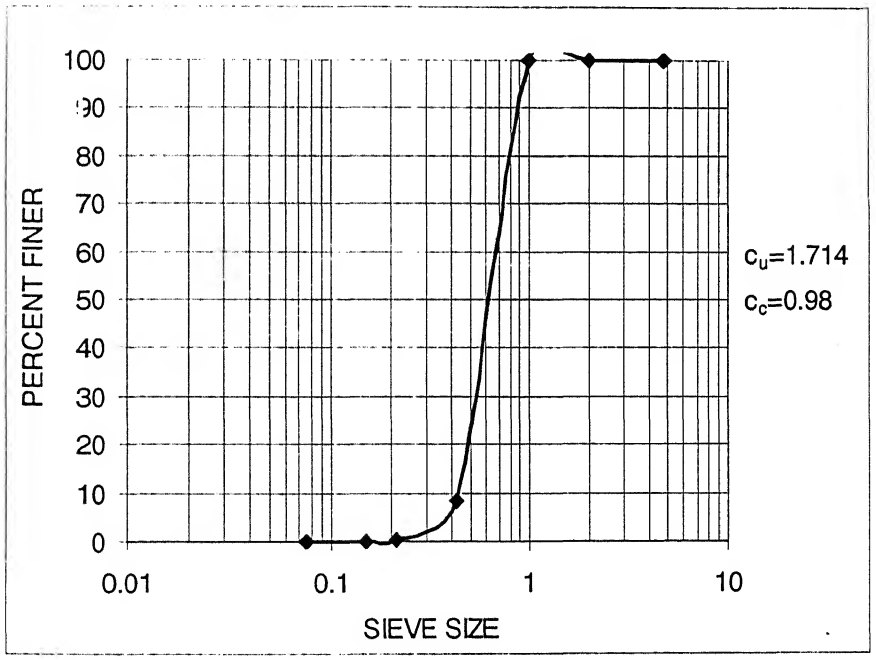

Figure 3.3 Grain distribution curve for standard grade-II Ennore sand

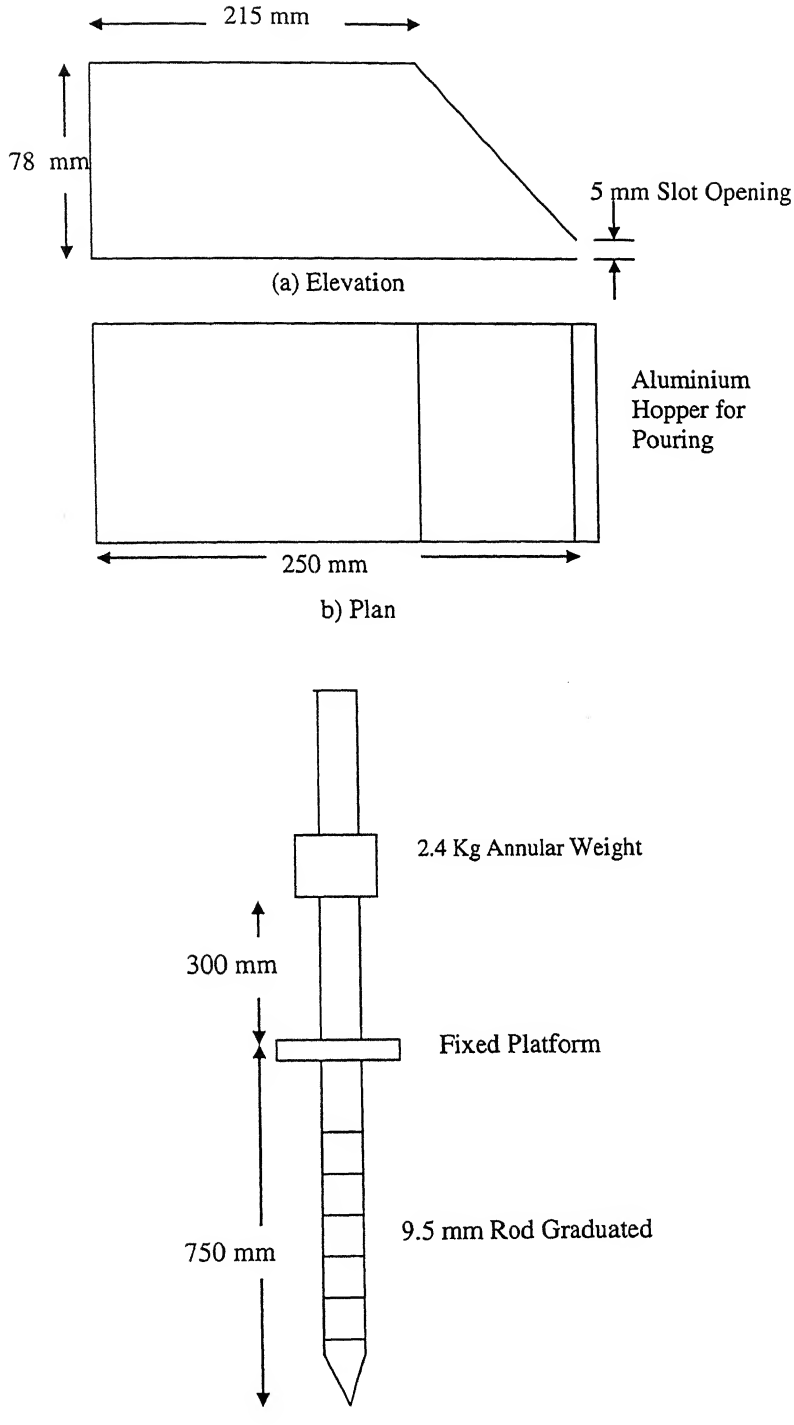

Figure 3.4 a) The elevation b) Plan view of hopper and c) Penetrometer

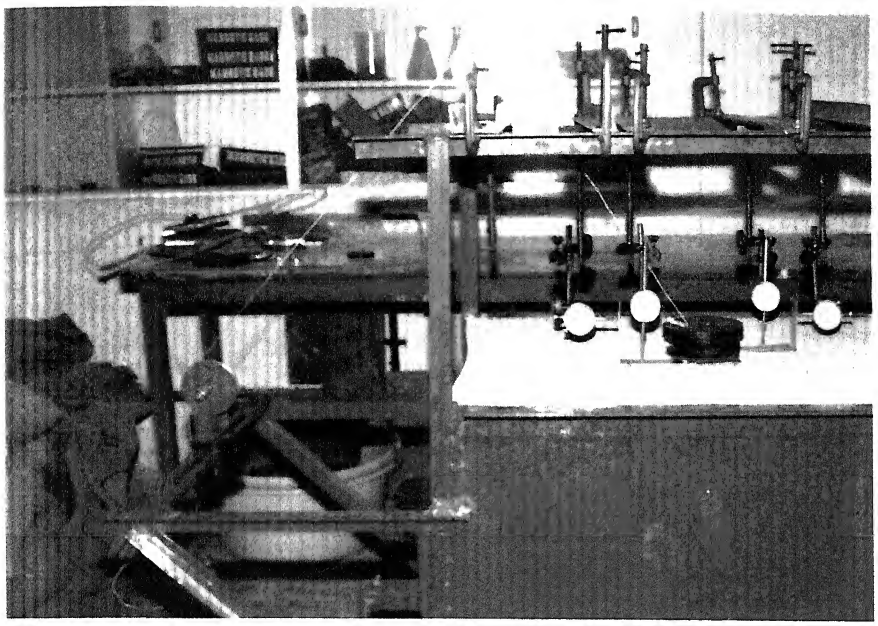

Plate No. 3.1 Complete experimental setup

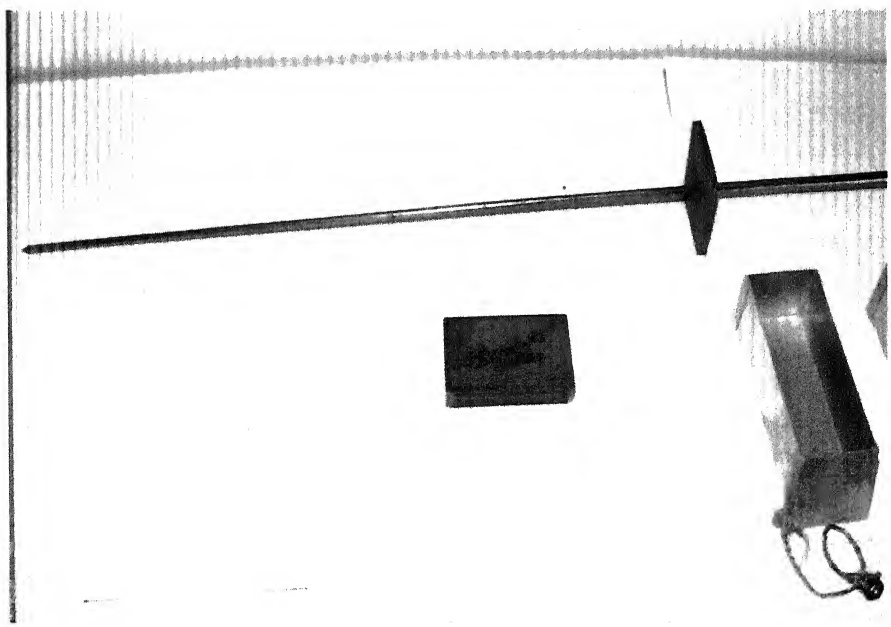

Plate No. 3.2 Hoppers and Dynamic penetrometer

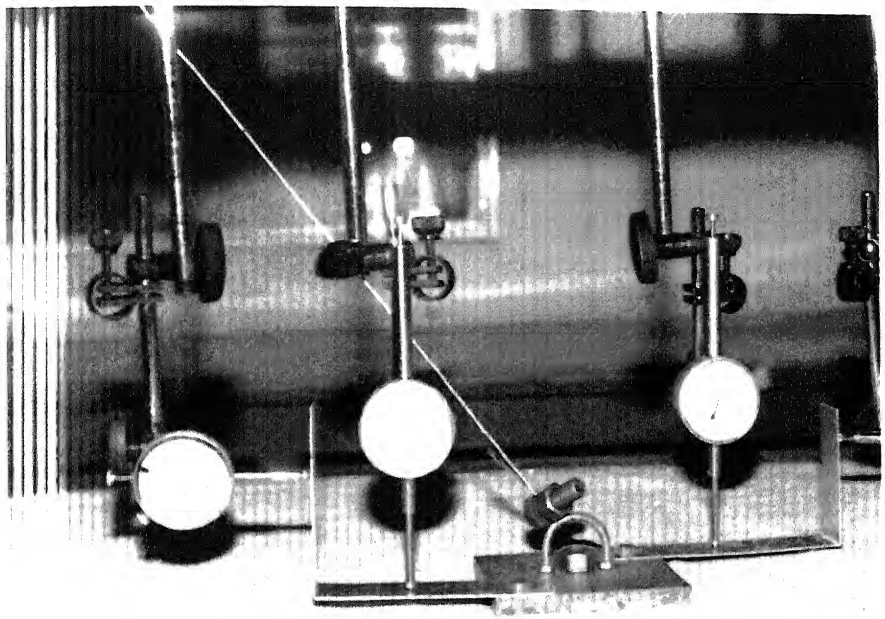

Plate No. 3.3 Placement of dial gauges

Plate No. 3.4 Sand pouring technique through Hopper

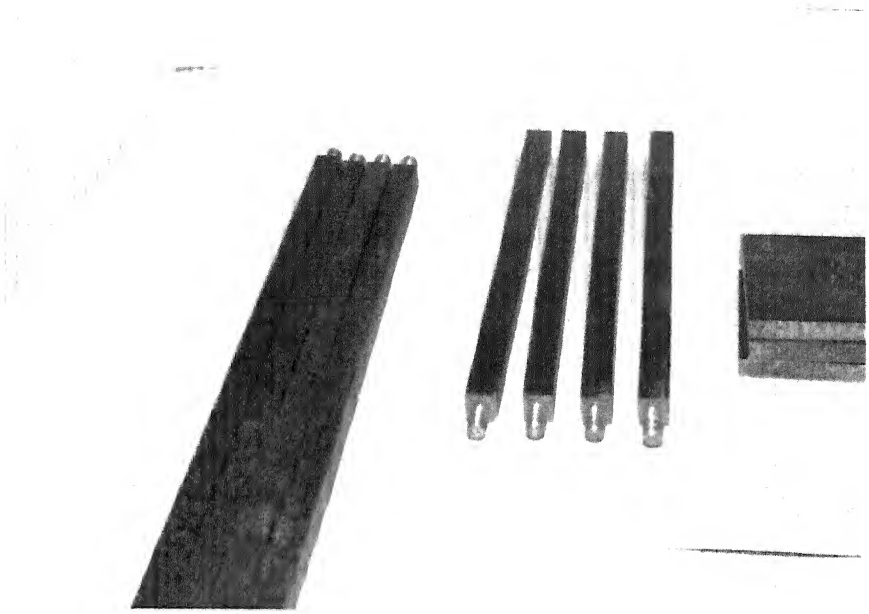

Plate No. 3.5 Piles and pile caps

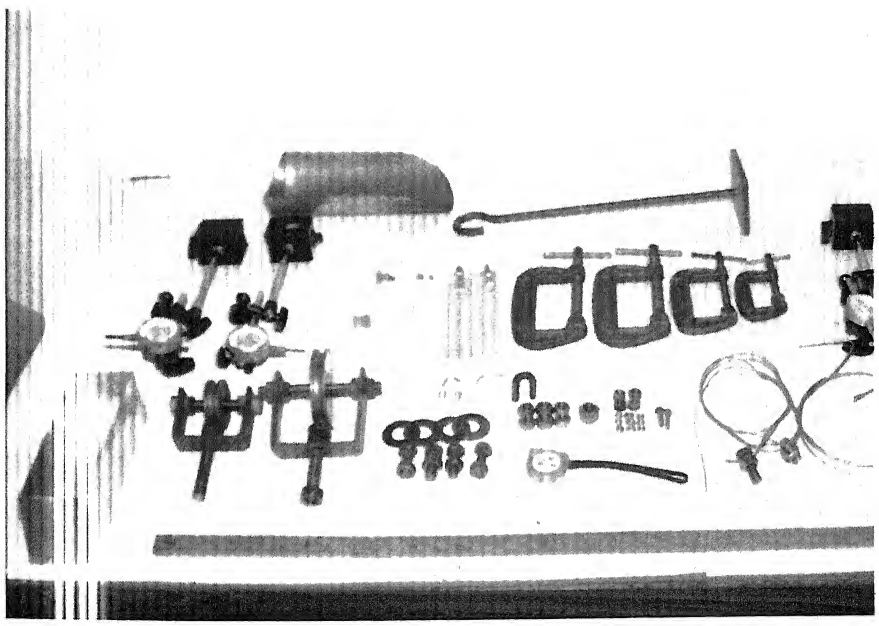

Plate No. 3.6 Experimental accessories

Chapter IV

Experimental Results and Discussions

4. 1 Introduction

Model uplift tests on single piles having L/d ratio 20 and 30, under various stages of compressive loads (i.e. 0%, 25%, 50%, 75%, and 100% of their ultimate load in compression) and angle of inclinations (α) 0^0, 30^0, 60^0 and 90^0 with vertical, in medium dense sand were carried out in the laboratory. A total number of 42 tests were conducted in which, one test each in compression for L/d ratio 20 and 30 and the remaining 40 number of tests were conducted in tension for both the L/d ratios at different loading conditions and angle of inclinations.

4. 2. Load-Displacement Diagrams

The load-displacement responses are non-linear in nature and it has been discussed briefly in the following sub headings:

1). Piles under axial compression
2). Piles under oblique pull (without static compressive loads)
3). Piles under oblique pull (with static compressive loads).

4.2.1 Piles under axial compression

The model piles having L/d ratios 20 and 30 were loaded vertically with gradual increment of loads and the corresponding load-displacement curves were obtained. The load-displacement diagram for L/d =20 and 30 in compression is shown in Figure 4.1. From Figure 4.1 at initial stage of the loading the load-displacement response is linear but afterwards it is non-linear. This series of tests were meant for the assessment of the ultimate load carrying capacity of piles in compression. The criterion for establishing the gross ultimate load from load-displacement diagrams has been discussed by Poulous and Davis (1980). The point where the load-displacement curve exhibits a peak or maintains a continuous displacement increase with no further increase in load is generally taken as the failure.

maintains a continuous displacement increase with no further increase in load is generally taken as the failure.

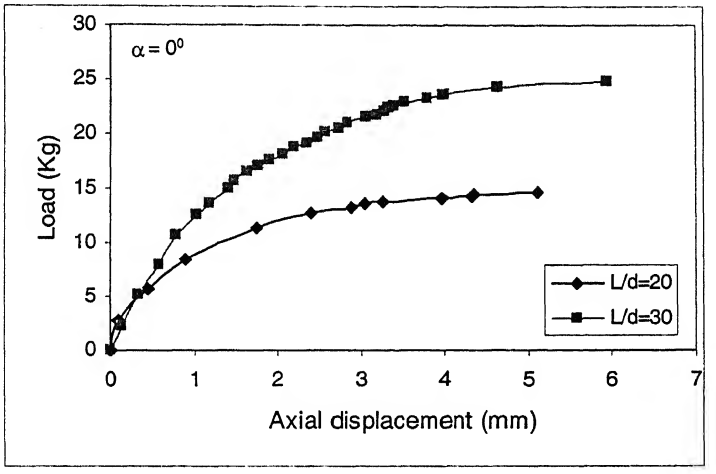

Figure 4.1 Load-displacement curves in compression.

4.2.2 Piles under Oblique pull (without static compressive loads)

In this section the load-displacement responses have been discussed under $\alpha=0^0$, $\alpha= 30^0$ & 60^0 and $\alpha=90^0$ conditions.

a) $\alpha = 0^0$ Condition

A typical diagram of pull versus axial displacement of piles under pure uplift condition has been shown in Figure 4.2. The initial part of the load-displacement curves is nearly linear and afterwards nonlinearity follows. It is observed that for different embedment lengths of piles, the axial movement of 0.15 d to 0.25 d is required to mobilize the ultimate uplift resistance. From the load-displacement response the gross ultimate load was taken to be the load at which the load-displacement curve becomes asymptotic to the displacement axis. At a particular displacement the uplift capacity increases with the in crease in embedment length of piles. It is about 50-70% higher for L/d= 30, compared to L/d=20.

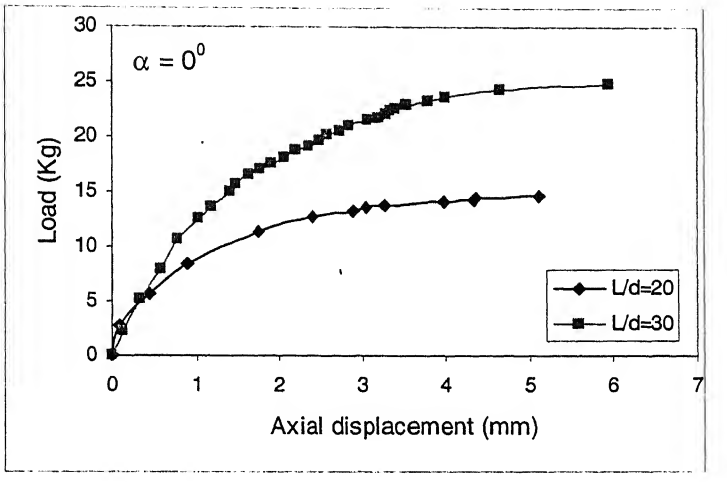

Figure4.2 Load-displacement curves in tension (0% compressive load)

b) $\alpha = 30^0$ & 60^0condition

Three types of load-displacement curves were plotted for the piles under oblique pull ($\alpha = 30^0$ and $\alpha = 60^0$ conditions). They are pull versus axial displacement, pull versus normal/ lateral displacement and pull versus rotation. Typical diagrams of oblique pull-axial displacement, oblique pull-normal displacement and oblique pull-rotation are shown in Figure 4.3. It is observed that the axial failure occurred when the inclination of the applied load with respect to the vertical was 30^0 and the bending failure occurred for 60^0.

In the case of axial failure, the ultimate resistance is taken as the load at which the pile moves out of the soil. In the Bending failure, ultimate resistance is taken as the load at which a large displacement occurs for a small increment of applied load. For L/d=20 and oblique pull inclination of 30^0, the axial failure occurred at a pile head displacement of 0.15d to 0.3d, whereas for L/d=30 it occurs at 0.2d to 0.4d. When inclination is 60^0, the bending failure occurred at a pile head displacement of 0.3d to 0.45d in case of L/d=20 and 0.6d to 0.7d for L/d=30.

The rotation failure occurred at a rotation of 0.5^0 to 1.5^0 for L/d=20, and 2^0 to 3^0 for L/d=30.

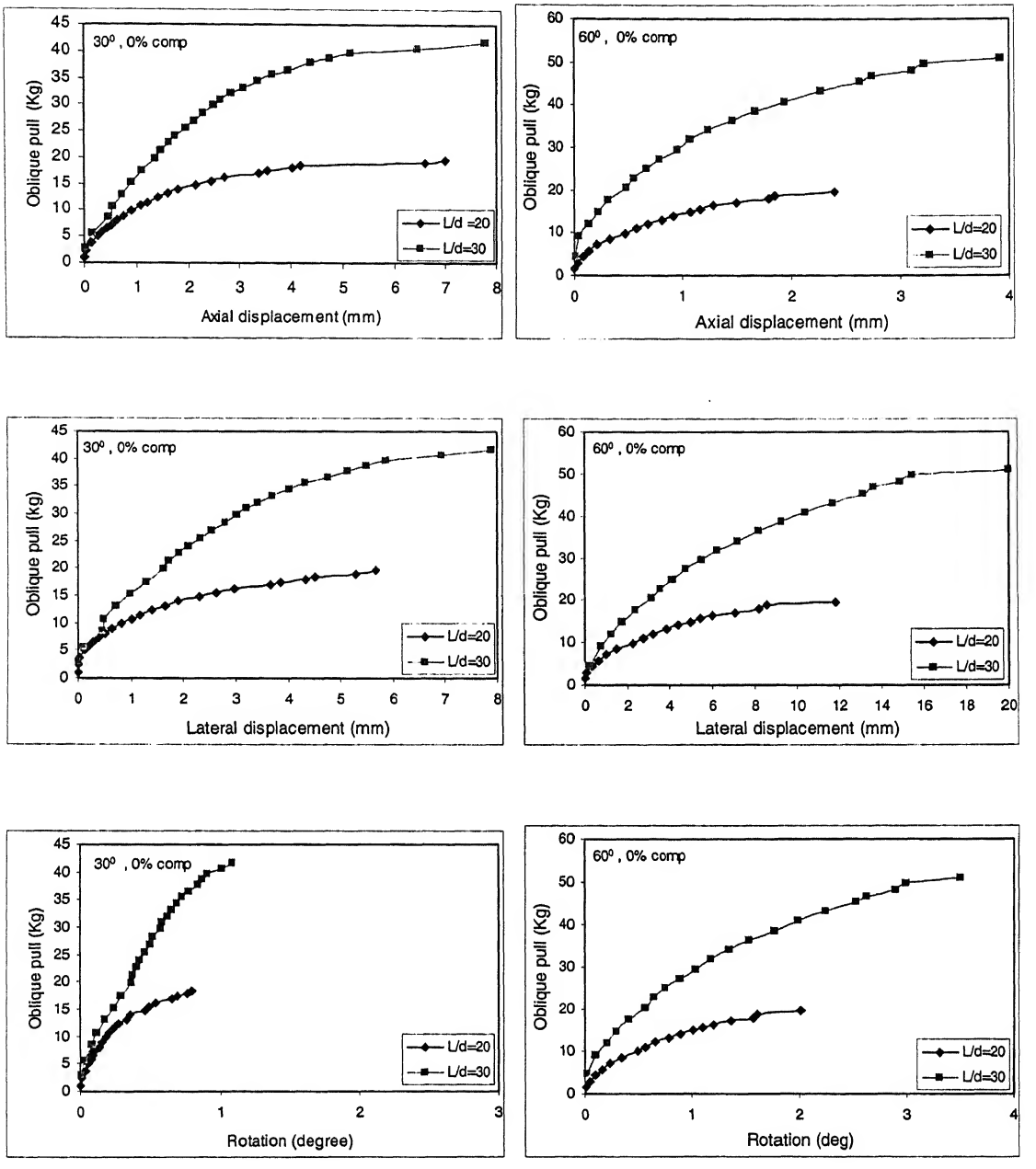

Figure 4.3 Oblique pull-Axial displacement and Oblique pull-Lateral displacement

c) $\alpha = 90^0$ condition

At $\alpha = 90^0$ condition, the axial displacement and rotation of the pile head are negligible as compared to the lateral displacement. Typical graph of pull vs lateral displacement is shown in Figure 4.4. The bending/lateral failure occurred at a pile head displacement of 0.3d to 0.5d. As the L/d ratio increases the oblique pull also increases due to increase in length of embedment.

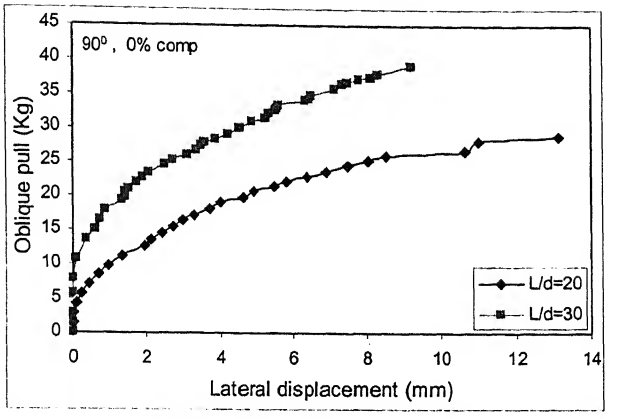

Figure 4.4 Oblique pull vs lateral displacement

4.2.3 Piles under oblique pull (with static compressive loads)

The test results of the model single piles in medium dense sand under various static compressive loads and inclinations of loads are shown in Figure 4.5-4.8. The piles exhibited a more nonlinear load-displacement behavior in uplift than in compression, due to the release of residual load, which was released from the tip resistance of piles as they were tensioned (O' Neill et. al 1982).

The load displacement behavior of piles subjected to different % of compressive loading conditions under different inclinations has been discussed in this section.

i) $a = 0^0$ Condition

Typical load-displacement curves of piles in axial condition subjected to different %of compressive loads are shown in Figure 4.5. For a particular L/d ratio, the applied load increases with increase in % of compressive loads. The axial failure occurred at a pile head displacement of 0.15d to 0.25d for L/d = 20 and 0.2d to 0.4d for L/d = 30.

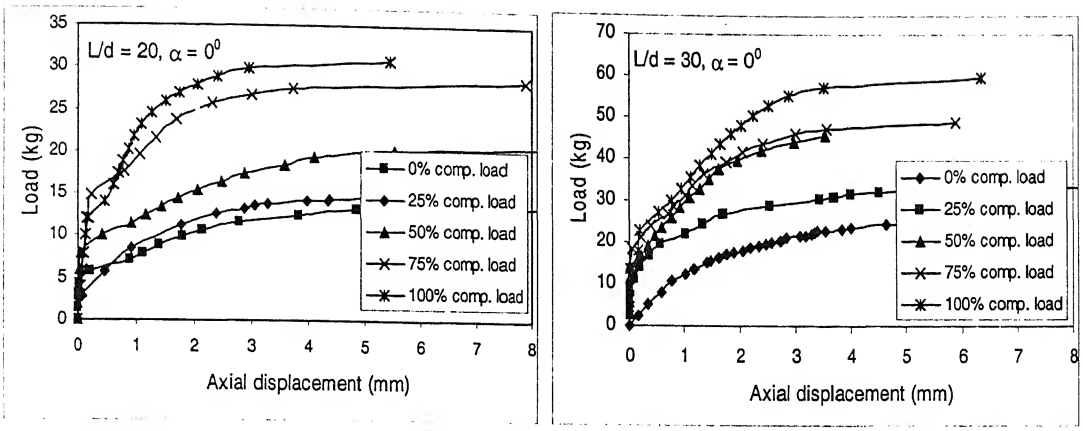

(a) L/d=20 (b) L/d=30

Figure 4.5 Load vs axial displacement curves for different compressive load cases ($\alpha=0^0$)

ii) $\alpha = 30^0$ & 60^0condition

The load-displacement response of piles under oblique condition for both the L/d ratios and for different % of compressive loading cases has been plotted and was shown in Figure 4.6, 4.7. In this three types of load-displacement curves are drawn they are

1). Oblique pull vs Axial displacement
2). Oblique pull vs Lateral displacement
3). Oblique pull vs Rotation.

The gross ultimate loads were determined from the load-displacement diagrams by investigating the region where a large displacement was derived for a small increment of applied load. It may be observed that the axial failure occurred in the case where the inclination of the applied load with respect to the vertical axis of pile $\alpha=30^0$ and the lateral type failure occurred f.or $\alpha=60^0$. From Figures 4.6, 4.7 it is observed that the axial failure occurred at $\alpha=30^0$ condition at a pile head displacement of 0.15d to 0.3d (i.e. 2mm to 8mm) for L/d ratio 20 and 0.15d to 0.4d (i. e. 3mm to 8mm) for in L/d ratio 30. However, for $\alpha=60^0$ condition the lateral failure occurred at a pile head displacement of 0.3d to d (6mm to 12mm) in case of L/d ratio 20 and 0.6d to d (12mm to 20mm) in case of L/d=30. From the load-displacement curves it is observed that as the compressive load increases, the lateral displacement is increasing as compared to the axial displacement. For 100% compressive load, the axial displacement to oblique

is negligible as compared to lateral displacement. Again as the % of compressive load increases to 100%, the failure mode occurred in lateral displacement of the pile.

The rotation failure occurred at a rotation of 1^0 to 2^0 for L/d=20 and 2^0 to 3^0 for L/d=30.

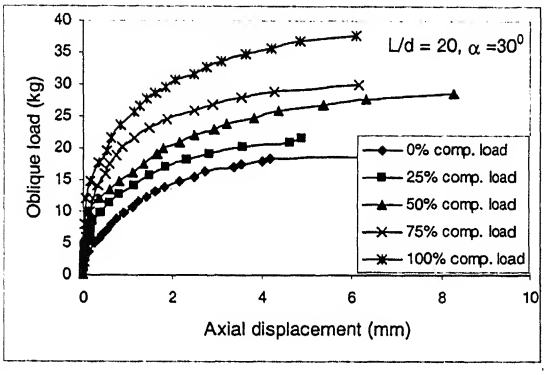

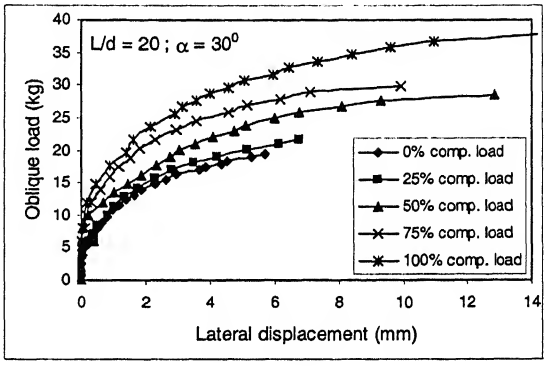

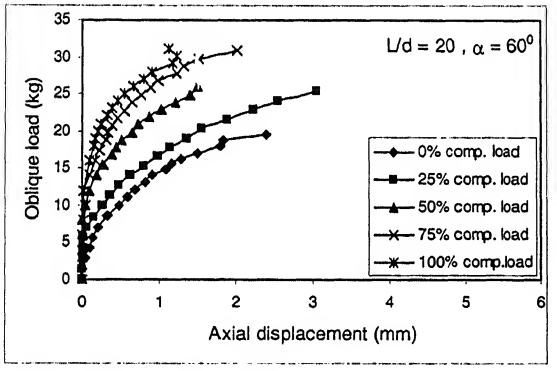

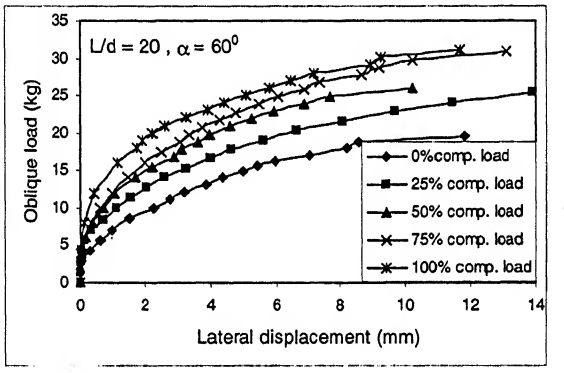

(a) Axial displacements for $\alpha = 30^0, 60^0$ (b) Lateral displacements for $\alpha = 30^0, 60^0$

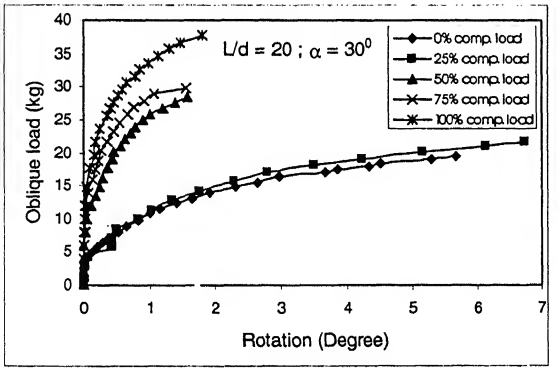

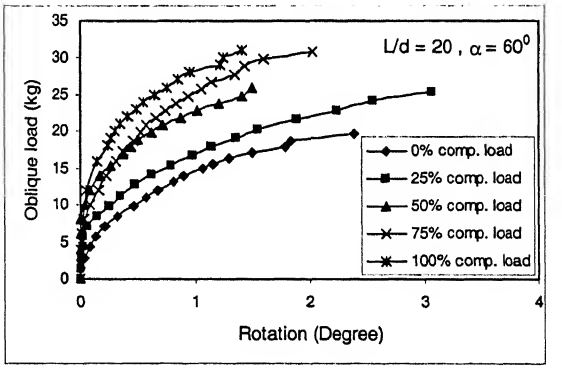

(c) Pull vs rotation for $\alpha = 30^0$ (d) Pull vs rotation for $\alpha = 60^0$

Figure 4.6 Oblique pull vs axial, lateral and rotational displacements (L/d=20)

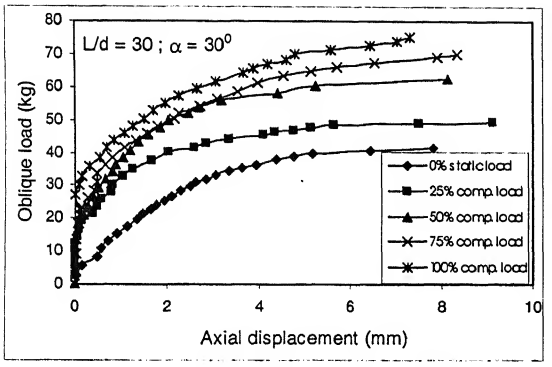

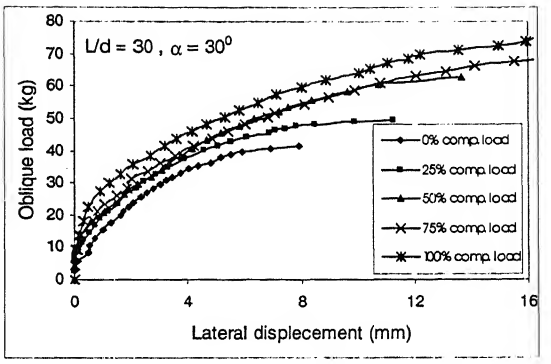

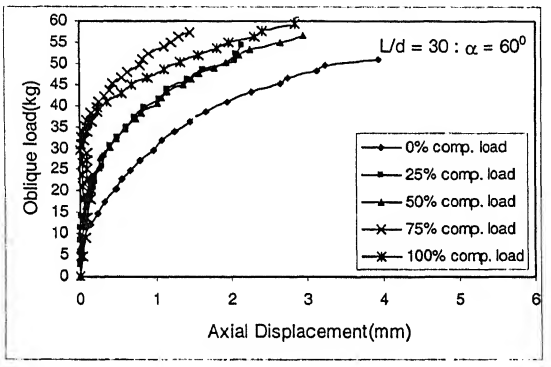

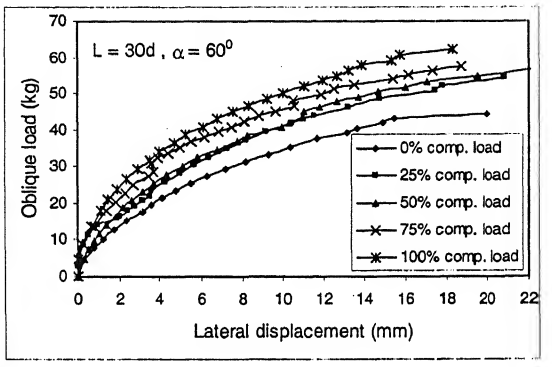

(a) Axial displacements for $\alpha = 30^0, 60^0$ (b) Lateral displacements for $\alpha = 30^0, 60^0$

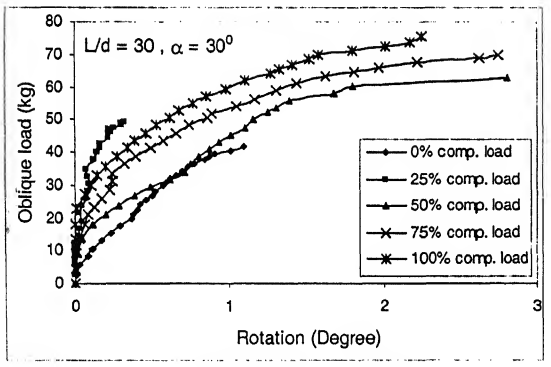

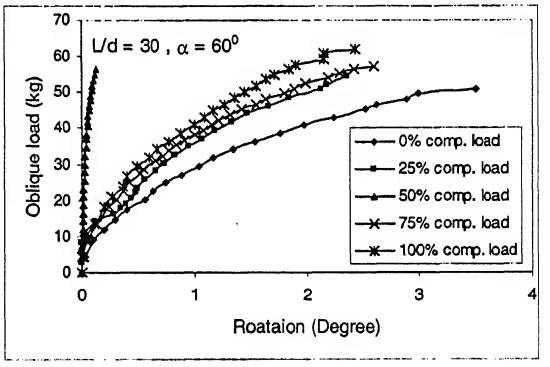

(c) Pull vs rotation for $\alpha = 30^0$ (d) Pull vs rotation for $\alpha = 60^0$

Figure 4.7 Oblique pull vs axial, lateral and rotational displacements (L/d=30)

iii) $\alpha = 90^0$ condition:

Typical graphs of lateral load-lateral displacement for different % of compressive loads have been shown in Figure 4.8. In the case of lateral condition as the percentage of compressive loading increases the axial displacements are negligible as compared with the lateral displacements. The rotation is also considered as negligible because the eccentricity of the load application is very negligible. The Ultimate lateral resistance is taken from load-lateral displacement diagrams by investigating the region where a large displacement was occurred for a small increment of applied load. It

occurred at a pile head displacement of 0.3 d to 0.6 d (i. e. 6 mm to 12 mm) in case of L/d ratio 20 whereas 0.5 d to d (i. e 10 mm to 16 mm) for L/d ratio 30.

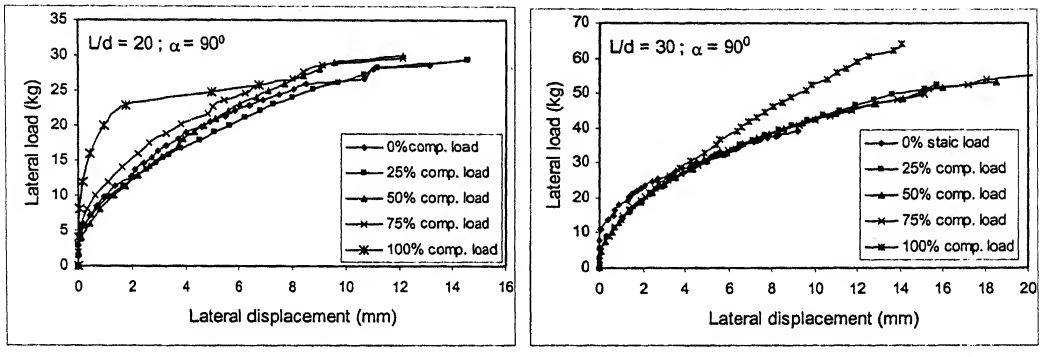

(a) L/d=20 (b) L/d=30

Figure 4.8 Lateral load vs lateral displacement

4.3 Ultimate Resistance

The ultimate resistance of piles under different loading conditions has been discussed in this section.

4.3.1 Piles under Axial pull

The ultimate resistance of the piles under axial pull has been estimated from the load vs axial displacement diagrams. It is taken as the load at which the pile moves out of the soil. In such condition the pull versus axial movement curves becomes parallel to the displacement axis and maintains continuous displacement with no further increase in pull.

4.3.2 Piles under Oblique pull

The ultimate resistance of the piles under oblique pull ($\alpha=30^0$ and $\alpha=60^0$) condition has been estimated from the oblique pull versus axial, normal and rotation diagrams. The minimum load obtained from these diagrams is taken as the ultimate resistance. In the case of axial failure, the ultimate resistance is taken as the load at which the pile moves out of the soil. In Bending failure, the ultimate resistance is taken from load-lateral displacement diagrams where a large displacement was occurred for a small increment of applied load.

4.3 3 Piles under Normal/Lateral pull

The ultimate resistance of the piles under lateral pull has been estimated from the load versus normal/lateral displacement diagrams. It is taken as the point where an addition of small load increment results large displacement.

The ultimate resistance has been given in Table 4.1.

Table 4.1 Ultimate resistance of piles

S. No.	Inclination (α)	% of stages of compressive load	L/d = 20	L/d=30
			Ultimate load(kg)	Ultimate load (kg)
1	0^0	0%	14.45	23.64
2		25%	15.31	28.98
3		50%	17.72	33.57
4		75%	20	39.18
5		100%	23	44.5
6	30^0	0%	18.39	39.65
7		25%	20.12	44.18
8		50%	22.02	49.89
9		75%	24.52	51.91
10		100%	26.65	57.26
11	60^0	0%	18.63	36.29
12		25%	19.06	37.15
13		50%	21.84	38.24
14		75%	24.76	43.68
15		100%	27.04	46.71
16	90^0	0%	25.81	42.57
17		25%	28.36	46.48
19		50%	29.03	51.51
20		75%	28.68	54.01
21		100%	22.82	60.51

4.4 Failure modes

Generally the mode of failure, axial or bending is decided from the load-displacement curves. The minimum load obtained from the pull versus axial displacement, pull versus normal displacement, pull versus rotation diagrams is taken as the ultimate oblique load and the failure mode is referred as either axial or bending. To confirm the failure mode further and to study the influence of the axial component on bending failure and normal component on axial failure, the ultimate oblique capacity (P_α) and its axial component (P_{Af}) and normal component (P_{Nf}) have also been drawn against the angle of inclination (α). The results have been presented through Figures 4.9 and 4.10. The values of the net axial uplift capacity (P_{nu}) and ultimate lateral resistance (P_L) which are known from the experimental results are also shown in these figures. The failure modes of the piles are discussed below.

1) Axial failure occurs when the axial component of the ultimate oblique load is greater than or equal to the net ultimate axial capacity, viz.,

$$P_{Af} \geq P_{nu}$$

Where

P_{nu} = net axial uplift capacity of pile

$P_{Af} = P_\alpha \cos \alpha$ = axial component ultimate oblique capacity

α = angle of inclination of load from vertical

2) Lateral failure occurs when the lateral component of the net ultimate oblique capacity is greater than or equal to the ultimate lateral resistance. Viz.,

$$P_{Nf} \geq P_L$$

From Figure 4.9 and 4.10, it has been observed that for piles of L/d=20 and L/d=30 subjected to different percentage of compressive loadings conditions, the axial failure occurred at $\alpha \leq 30^0$ and bending failure for $\alpha \geq 60^0$. The axial failure is associated with the axial component of pull P_{Af}, being equal or greater than the axial uplift capacity P_U of the pile. During bending failure, the normal component P_{Nf} at failure is less than the ultimate lateral resistance, P_L, indicating that the presence of the axial component and rotation of pile head influence the normal load carrying capacity.

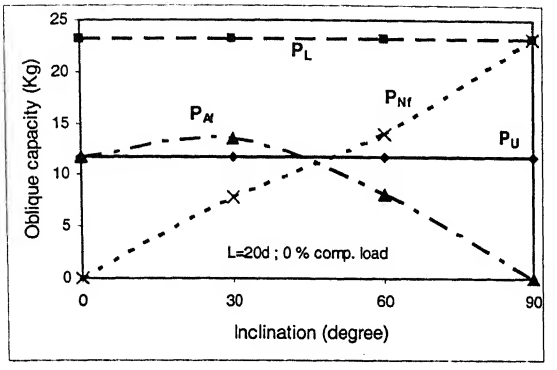

(a) 0% comp. load

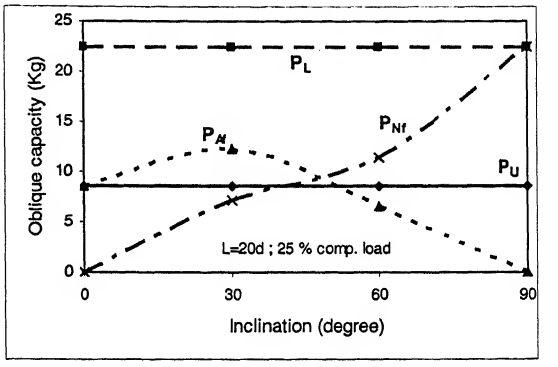

(b). 25% comp. load

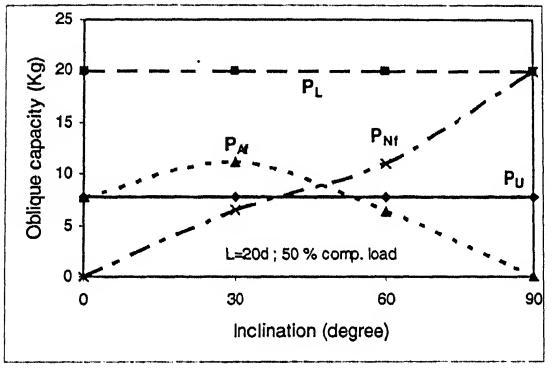

(c) 50% comp. load

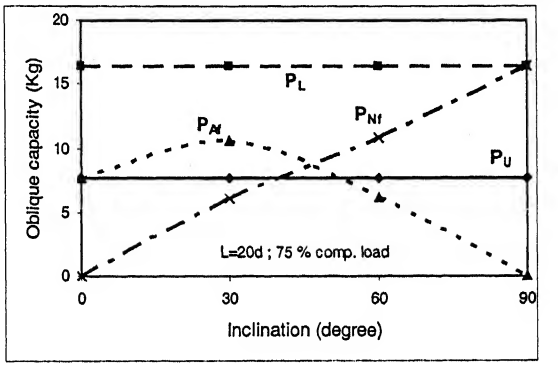

(d) 75% comp. load

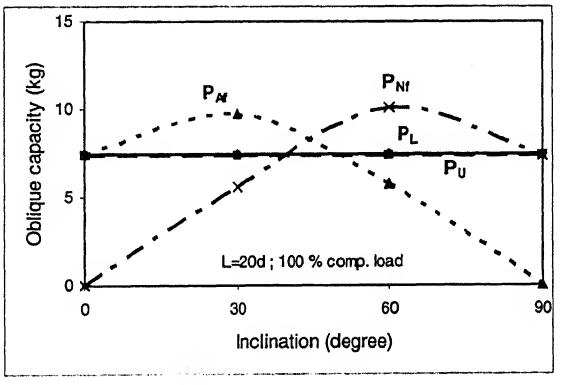

(e) 100% comp. load

Figure 4. 9 Oblique capacity vs inclination (L/d=20)

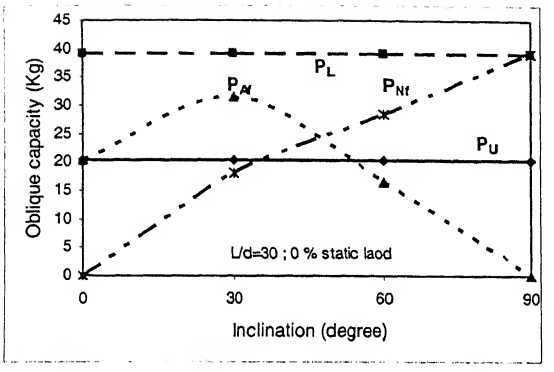

(a) 0% comp. load

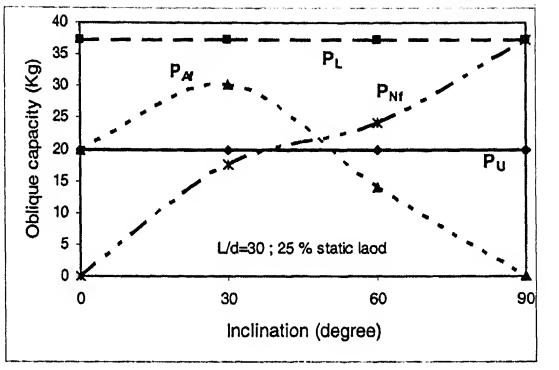

(b) 25% comp. load

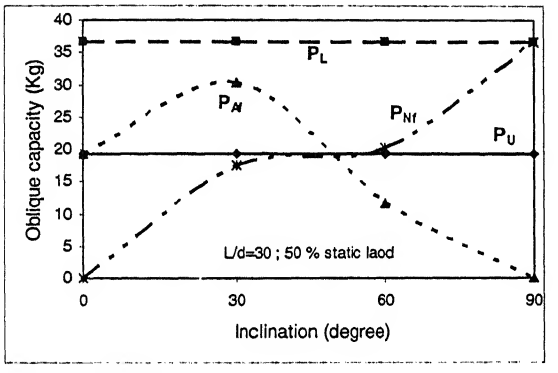

(c) 50% comp. load

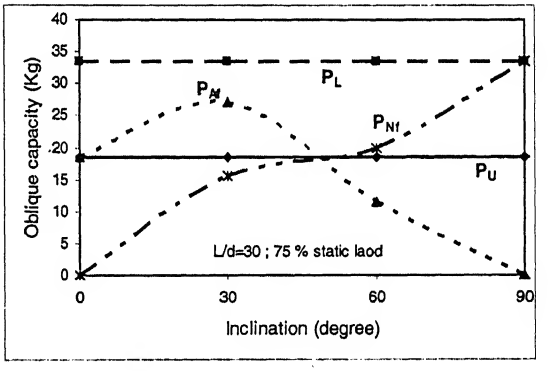

(d) 0% comp. load

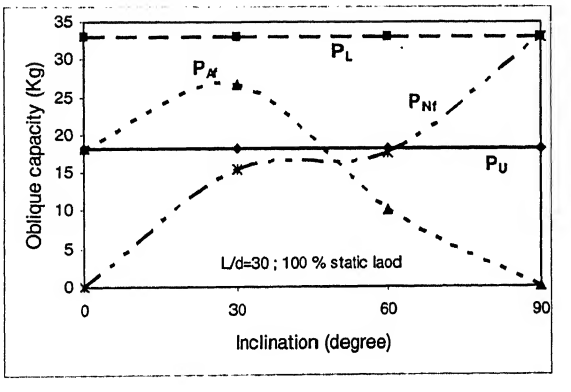

(e) 100% comp. load

Figure 4.10 Oblique capacity vs Inclination (L/d=30)

4.5 Variation of oblique capacity with percentage of compressive load

The variation of oblique pullout capacity of single piles having L/d ratio 20 and 30, subjected to different percentage of ultimate load in compression has been discussed below.

4.5.1 $\alpha=0^0$ Condition

In axial condition, for L/d ratio 20 and 30 the net axial uplift capacity of piles decreases as the percentage of compressive load increases. At initial stages the decrease is about 25% afterwards the decrease is marginal for the case of L/d ratio 20. However the decrease is marginal through out the variation of compressive loading for L/d ratio 30. The percentage decrease in net uplift capacity for particular L/d ratio with % of compressive loading is given in the following Table 4.2.

Table 4.2 Variation of net uplift capacity with % of compressive load ($\alpha=0^0$)

	0-25%	25-50%	50-75%	75-100%
L/d=20	27.69%	8%	2.39%	2.45%
L/d=30	2.42%	3.0%	3.1%	2.31%

The variation of net axial uplift capacity with percentage of compressive loading is shown in Figure 4.11. The similar trend was observed by Dash and Pise (2003). This is because due to the placement of compressive load on the pile may result in a change in soil fabric at the pile soil interface of the pile. Moreover as the pile gets pushed inside the soil under the action of static compressive load, it is assumed that there is no densification of the sand surrounding the pile. So, the effect of compressive load on pile only alters the soil pile friction angle δ. The soil friction angle φ remains unchanged. For a particular static loading condition the variation of net uplift capacity increases with increase in L/d ratio. The variation for 0%, 25%, 50%, 75%, and 100% is 42.0%, 57.0%, 59.14%, 58.9% and 59.0% respectively.

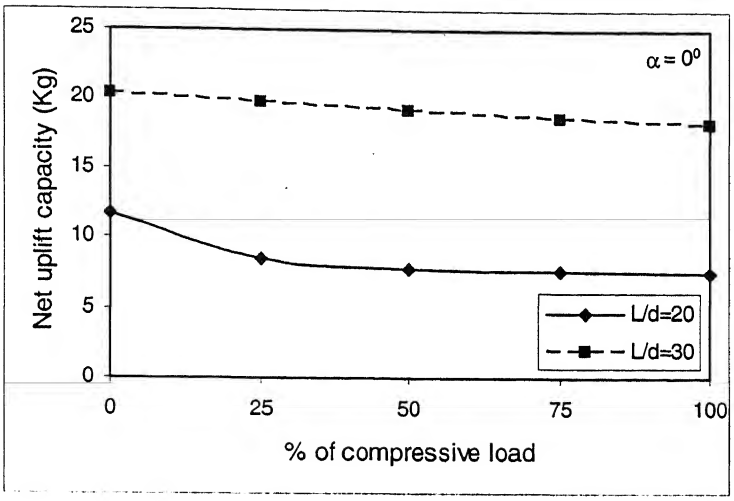

Figure 4.11 Net uplift capacity vs % of compressive load (L/d=20 & 30, $\alpha=0^0$)

From Figure 4.11 it is to be observed that the net uplift capacity is constant after 50% of stage loading. That means the stage loading has no effect on uplift capacity of piles after 50% of compressive loads.

4.5.2 $\alpha=30^0$ Condition

In 30^0condition, for L/d ratio 20, the oblique capacity decreases gradually with increase in percentage of compressive load. For L/d ratio 30 the oblique capacity decreases gradually up to 50% of ultimate load in compression afterwards the decrease is more and about 10% lower than the capacity at 50% of compressive load. The variations are shown in Table 4.3.

Table 4.3 variation oblique capacity with % of compressive load ($\alpha=30^0$)

	0-25%	25-50%	50-75%	75-100%
L/d=20	9.31%	9.02%	5.31%	8.62%
L/d=30	3.5%	0.11%	10.6%	1.3%

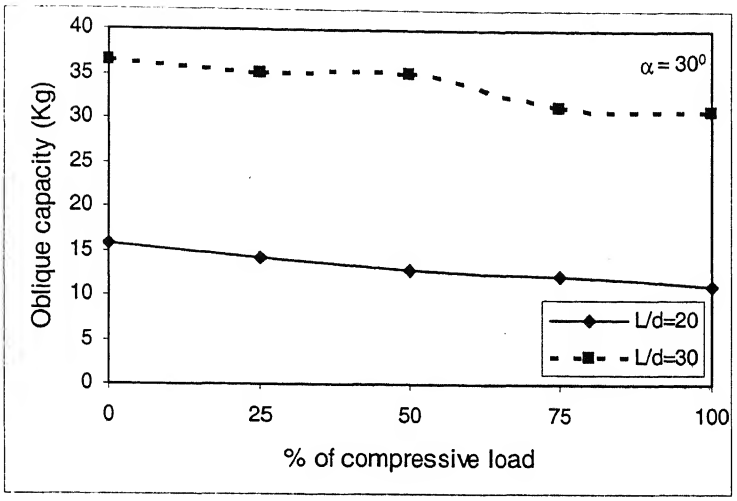

Figure 4.12 Oblique capacity vs % of compressive load (L/d=20 & 30, $\alpha=30^0$)

The variation of oblique capacity with percentage of compressive loading for 30^0condition is shown in Figure 4.12. For a particular compressive loading condition the percentage increase in oblique capacity increases with increase in L/d ratio of the pile. The variation is 0%, 25%, 50%, 75%, and 100% is 56.77%, 59.38%, 63.0%, 60.7% and 63.7% respectively.

4.5.3 $\alpha=60^0$ Condition

In 60^0condition, for L/d ratio 20 the oblique capacity decreases gradually with increase in % of compressive load. For L/d ratio 30 the decrease in oblique capacity is about 15 % as the compressive load increases up to 50%. However, the variation is gradual afterwards. The percentage of variation of oblique capacity is shown in Table 4.4.

Table 4.4 variation oblique capacity with % of compressive load ($\alpha=60^0$)

	0-25%	25-50%	50-75%	75-100%
L/d=20	17.97%	3.14%	2.03%	7.16%
L/d=30	14.8%	16.6%	1.30%	11.8%

The variation of oblique capacity with % of compressive loading for 60^0condition is shown in Figure 4.13. For a particular compressive loading condition the percentage increase in oblique capacity increases with increase in L/d ratio of the

pile. The variation is 0%, 25%, 50%, 75%, and 100% is 51.18%, 52.97%, 45.36%, 45.76% and 42.97% respectively.

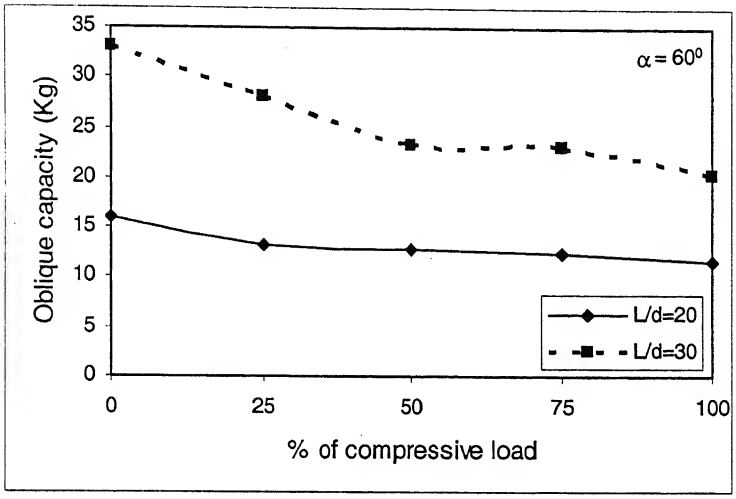

Figure 4.13 Oblique capacity vs % of compressive load (L/d=20 & 30, $\alpha=60^0$)

Form the Figure 4.13 it is observed that for 60^0condition the effect of % of compressive load is negligible on oblique capacity of piles having L/d=20.

4.5.4 $\alpha=90^0$ Condition

In lateral condition, for both the L/d ratios the lateral capacity decreases gradually as the percentage of compressive load increases (shown in Figure 4.14). At initial stages the decreasing rate is marginal for both L/d ratios of pile afterwards the decrease is about 15 to 55% for L/d ratio 20 and about 8% for L/d ratio 30. The variation of lateral capacity with % of static load is shown in Table 4.5.

Table 4.5 variation lateral capacity with % of compressive load ($\alpha=90^0$)

	0-25%	25-50%	50-75%	75-100%
L/d=20	3.19%	11.2%	17.689%	55.05%
L/d=30	4.8%	1.9%	8.87%	1.1%

For a particular compressive loading condition the percentage increase in oblique capacity increases with increase in L/d ratio of the pile. The variation is 0%, 25%, 50%, 75%, and 100% is 40.8%, 39.8%, 45.5%, 50.79% and 77.62% respectively.

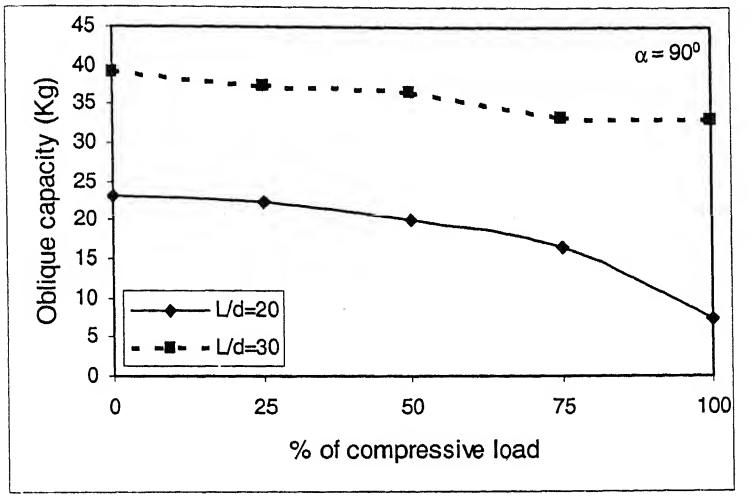

Figure 4.14 Lateral capacity vs % of compressive load (L/d=20 & 30, $\alpha=90^0$)

From the Figure 4.14 it is to be noted that in lateral condition the compressive load has no effect on oblique capacity of piles having L/d ratio 30.

4. 6 Polar Diagrams

When the value of a function changes with the direction, the function can be conveniently be represented through a polar diagram. In a polar diagram an origin called a pole is chosen and the direction is given by α, measured clockwise at the origin from a reference line through the origin. The value of the function is plotted radially from the origin along that direction. It is shown in Figure 4.15. To read the value of the function, $f(\alpha)$, for which ACB is the plotted curve, an angle α is measured from OA and a line OC is drawn. The value of function $f(\alpha)$ is given by OC. The presentation of ultimate resistance of piles to oblique pulling loads has been extensively done through polar diagrams by Meyerhof (1973a), Meyerhof (1973b), Meyerhof and Gopal Ranjan (1973), Meyerhof et al (1983), Chattopadhyay and Pise (1986), Patra (2001).

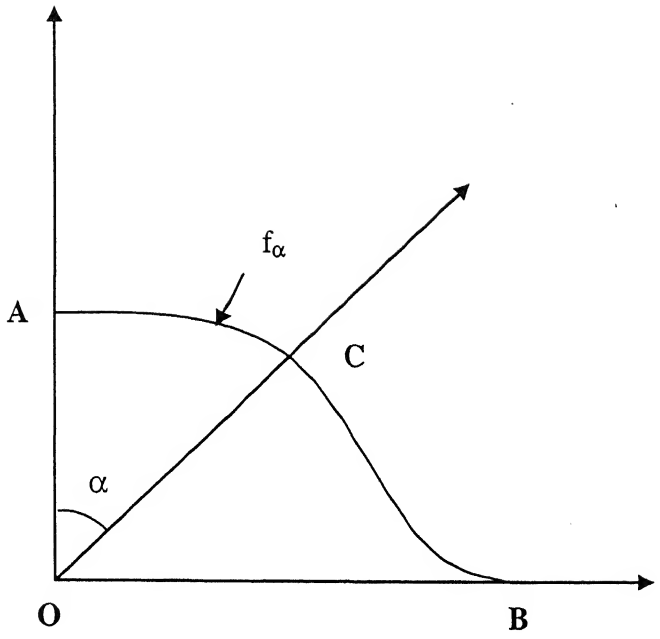

Figure 4.15 Polar diagram

Generally the advantage of the polar diagram to the oblique load is to know the compressive view of the effect of inclination of the load. As it is a continuous function it gives the inclination at which the pile offers maximum resistance that is called optimum resistance. Polar diagrams in a non-dimensional form give an idea quantitatively and qualitatively to the design engineers and field engineers to predict the ultimate resistance of piles under oblique pulling loads.

The ultimate resistance under oblique pull, P_α, of a pile has been expressed in non-dimensional form, P_α / P_U, in terms of the net axial uplift capacity, P_U, and ultimate lateral resistance, P_L, and the angle of inclination 'α'.

At $\alpha=0^0$, $P_\alpha/P_U=1 \Rightarrow P_\alpha=P_U$

At $\alpha=90^0$, $P_\alpha=P_L$

The value of P_α/P_U for different values of α and different values % of compressive loading cases are plotted for $P_U/P_L<1$. These plots are shown in Figure 4.16. The optimum resistance to oblique pull for different % of loading cases has been shown in Table 4.7

The test for model piles under various percentage of compressive loads and inclinations of the load are in shown in Figure 4.16 in the form of polar diagrams which gives the optimum resistance of the piles under oblique pull. The corresponding

relationships for the test results on single piles are shown in Figure 4.16 and indicate the optimum resistance for the cases of L/d=20 and L/d=30 occurs at an angle of inclination 90^0.

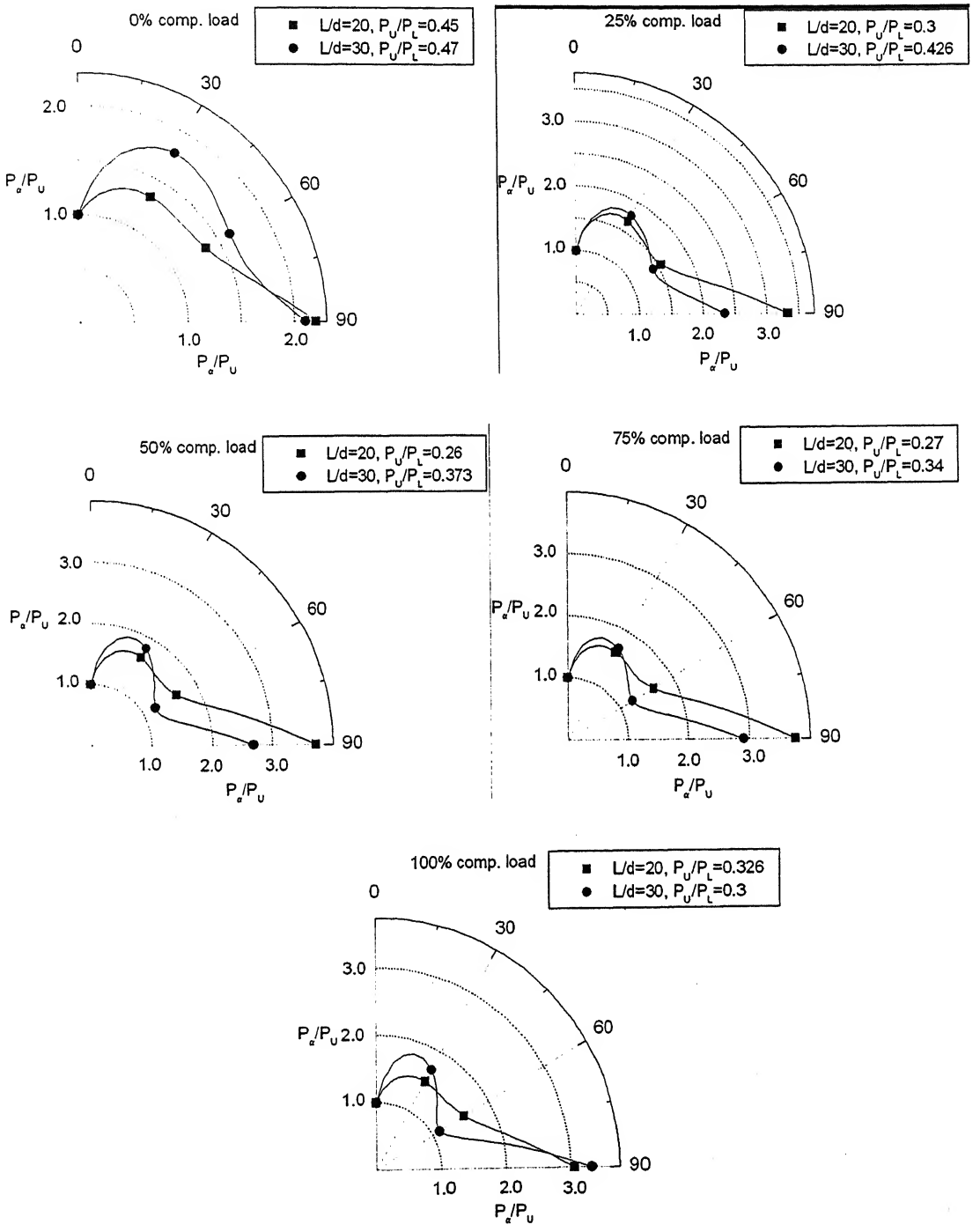

Figure 4.16 P_{α}/P_U vs inclination for L/d=20 & 30

Table 4.6 Optimum resistance of piles

	% of compressive load	Optimum resistance
L/d=20	0	90^0
	25	90^0
	50	90^0
	75	90^0
	100	90^0
L/d=30	0	90^0
	25	90^0
	50	90^0
	75	90^0
	100	90^0

Chapter V

Analysis

5.1 Introduction

No proper methods of analysis of piles under oblique pulling loads subjected to static compressive loads are available. In this chapter semi-empirical methods have been suggested to predict the ultimate oblique capacity of piles under static compressive loads.

Three semi-empirical methods have been suggested in the following form, viz.,

1. Ultimate axial uplift capacity of single piles under static compressive loads.
2. Ultimate lateral capacity of single piles under static compressive loads.
3. Ultimate oblique capacity of single piles under static compressive loads

5.2 Ultimate axial uplift capacity of single piles under static compressive loads

A semi empirical approach is suggested to evaluate the axial uplift capacity of piles under compressive load based on experimental results.

5.2.1 Calculation of shaft resistance

In the case of pure uplift condition (without compressive load) the net uplift capacity (Q_{nu}) comes from shaft resistance only, whereas the end bearing is non existent. It is theoretically expressed as follows:

$$P_{nu} = f_s A_s \qquad (5.1)$$

Where,

f_s = Skin friction of pile

A_s = surface area of the pile ($320cm^2$ for L/d=20, $480cm^2$ for L/d=30).

The skin frictional resistance, f_s, of the pile is calculated by substituting the experimentally determined P_{nu} values of different % of static compressive loads in the

Equation 5.1. Figure 5.1 shows the variation of f_s with % of static compressive load for different L/d ratios of the piles. As the static compressive load increases the f_s decreases and the decrease is gradual for L/d ratio 30 whereas for L/d ratio 20 it decreases drastically up to 25% of static load afterwards it is gradual. For a particular value of compressive load, as the L/d ratio increases, the f_s value also increases because of the increase in embedment length of the pile. The percentage increase in f_s for 0%, 25%, 50%, 75% and 100% of static load is 14.94, 55.14, 63.93, 63.02 and 62.66 respectively.

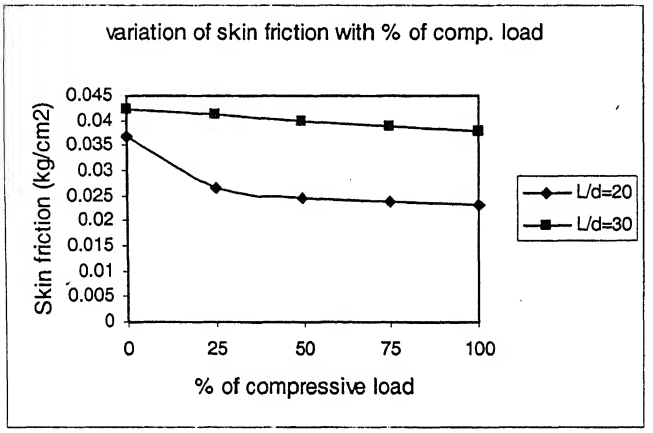

Figure 5.1 Shaft resistance vs % of compressive load.

5.2.2 Calculation of soil-pile friction angle (δ)

The soil-pile friction angle,δ, which is responsible for pure uplift is determined by means of direct shear test, which is of the order of 26.6^0. The placement of compressive load on pile may result in change in soil fabric at the pile-soil interface of the pile (Kraft 1991). And there is no densification of sand surrounding the pile. It is assumed that the effect of compressive load only alters the soil-pile friction angle.

Theoretically the f_s is calculated from the below equation.

$$f_s = (K_s \gamma z) \tan\delta \qquad (5.2)$$

Where,

K_s = Coefficient of lateral earth pressure

γ = Unit weight of soil

z = depth of the soil

δ = Soil-pile friction angle.

In the Equation 5.2, the product of K_s, γ and z will remain constant for different static compressive loads. The δ value is calculated for different static compressive loading conditions and for different L/d ratios, by substituting the values of f_s (computed in section 5.2.1) and product of K_s, γ and z in Equation 5.2. The computed values of δ for different static loading conditions were shown in Table 5.1. From Table 5.1 it is observed that the reduction in δ values increases with the increase in the stages of loading. Further it is observed that the reduction in soil-pile friction angle is more for L/d ratio 20 than is for L/d ratio 30.

Table 5.1 values of Soil-pile friction angle for different static compressive loads

	Soil-pile friction angle(δ)	
% of comp. load	L/d=20	L/d=30
0	26.6	26.6
25	18.88	24.79
50	17.46	24.12
75	17.06	23.43
100	16.67	22.95

5. 2. 3 Calculation of axial uplift capacity of piles

Chattopadhyay and Pise (1986a) have proposed a generalized theory to predict the net uplift capacity of pile under axial uplift load. Their approach is based on the suitable assumptions. The theory involves the soil-pile parameters such as length of a pile, L, diameter of a pile, d, angle of shearing resistance, ϕ, of sand and the soil-pile friction angle, δ. According to their method the net uplift capacity of a single pile is given by

$$P_{nu} = A_1 \pi \gamma d L^2 \qquad (5.3)$$

Where,

P_{nu} = net uplift capacity of a pile

L = depth of embedment of a pile

d = diameter of a pile

γ = effective unit weight of soil, and

A_1 is the net uplift capacity factor and is found from the chart given by Chattopadhyay and Pise (1986) shown in Figure 5.2. The net uplift capacity factors, A_1, are functions of ϕ, δ and λ=(L/d).

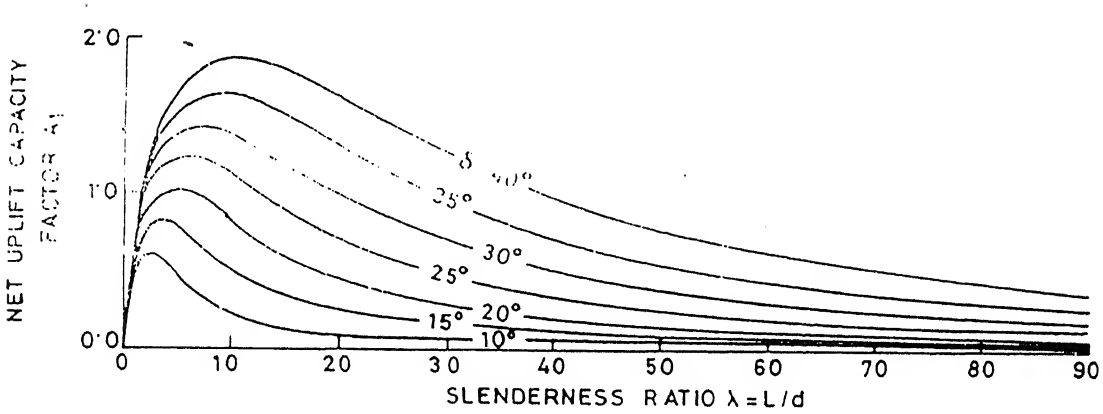

Figure 5.2 Net uplift capacity factor A_1 vs slenderness ratio (ϕ=40^0)

The above approach is for piles under axial uplift condition which has been extended to predict the net axial uplift capacity of piles under static compressive loading conditions.

The net uplift capacity factors for different static compressive loading are determined from the charts given by Chattopadhyay and Pise (1986) for the calculated values of soil-pile friction angles (shown in Table 5.1). The predicted values are shown in Table 5.2.

Table 5.2 Predicted net uplift capacity of piles

	Net uplift capacity (kg)	
% of compressive load	**L/d = 20**	**L/d = 30**
0	11.356	22.158
25	7.147	19.656
50	5.082	18.226
75	4.765	16.082
100	3.812	15.01

5.3 Ultimate lateral capacity of single piles under static compressive loads

The log-log method is extended to determine the ultimate lateral resistance of single piles subjected to static compressive loads. Applied lateral loads and the corresponding deflections for piles under different static compressive loads are plotted in log-log scale. Typical graphs were shown in Figure 5.3. In all cases the straight line relationship is generated. Ultimate loads for different static compressive loads are evaluated from the straight line relationships from the log-log plots corresponding to the deflection equal to the width of the piles. The predicted values are shown in Table 5.3.

Table 5.3 Predicted ultimate lateral capacity of piles

	Ultimate lateral capacity (Kg)	
% of compressive load	**L/d=20**	**L/d=30**
0	35	50
25	36	52
50	44	59
75	36.5	59
100	33	76

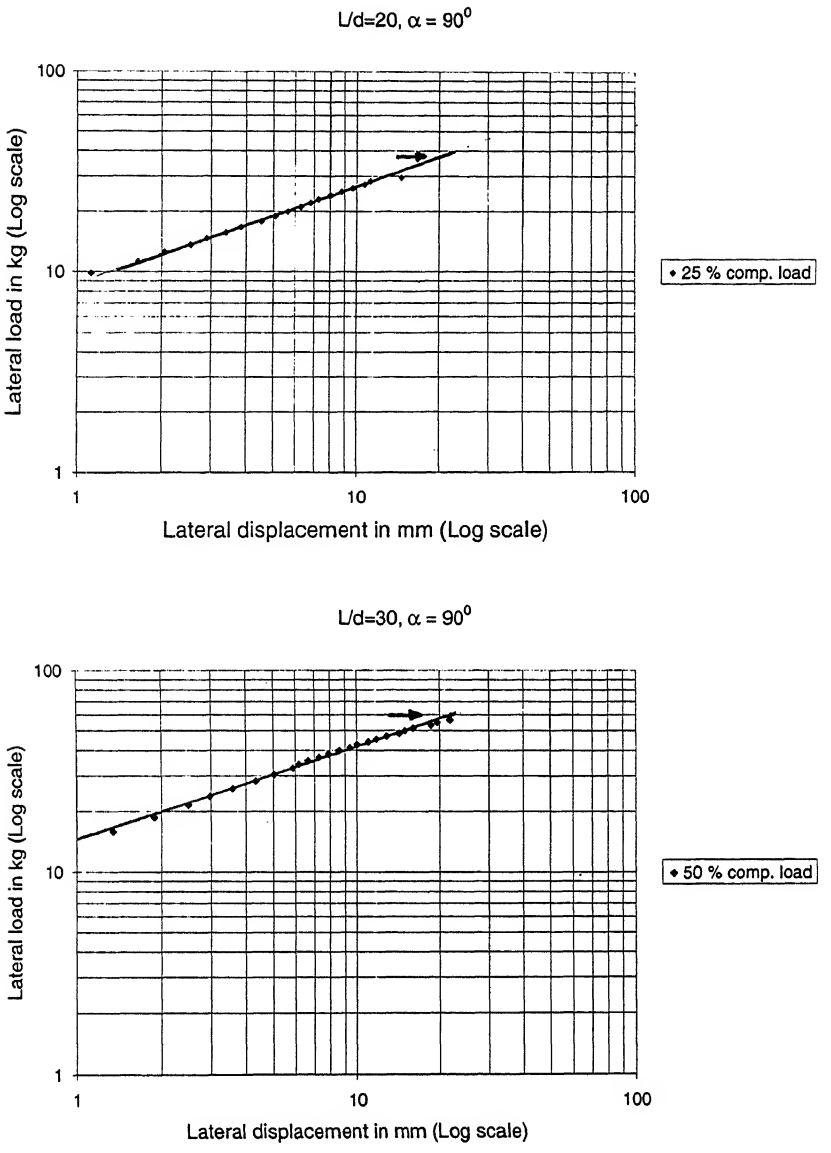

Figure 5.3 Lateral pull vs lateral displacement (Log-Log plot)

5.4 Ultimate oblique capacity of single piles under static compressive loads

A semi-empirical method has been proposed by Chattopadhyay and Pise (1986) to predict the ultimate oblique pulling resistance, P_α, in terms of $m = P_U/P_L$ and inclination of load, α.

$$P_\alpha = P_u \cos^2 \alpha \exp\left[-\left(\frac{1-m}{1+m}\right)\frac{\alpha^0}{90^0}\right] + P_L \sin \alpha \exp\left[-\left(\frac{1-m}{1+m}\right)\left(\frac{90^0-\alpha^0}{45^0}\right)\right] \quad (5.4)$$

Where,

α = Load inclination with vertical pile-axis

$P_u = P_{\alpha=0^0}$ = net ultimate uplift load for axial-pulling

$P_L = P_{\alpha=90^0}$ = ultimate resistance for horizontal pulling.

The above method has been extended to predict the ultimate oblique pulling resistance of pile under static compressive loads. The pre determined values of P_u and P_L from Section 5.2 and 5.3 respectively are substituted in Equation 5.4 to obtain the ultimate oblique capacity of piles subjected to static compressive loads. The Predicted values are shown in Table 5.4.

Table 5.4 Predicted ultimate oblique capacity of piles

% of compressive load	Predicted oblique capacity (kg)			
	$\theta = 30^0$		$\theta = 60^0$	
	L/d=20	L/d=30	L/d=20	L/d=30
0	19	33.43	21.6	35.5
25	19.13	37.257	21.3	39.217
50	20	42.79	23.13	44.958
75	22.5	47.01	24.13	48.755
100	28.81	53.7	25.9	56.647

Chapter VI

Comparison of Theoretical and Experimental Results

6.1 Introduction

Methods of analysis to estimate the ultimate axial capacity, the ultimate lateral resistance and the ultimate resistance of piles under oblique pull subjected to static compressive loads are presented in Chapter V. Results obtained from these analyses are compared with the present laboratory model test results and also with the results of other researchers in some specific cases.

Validity of any analysis can be established by the comparison with the experimental results. Few experimental results on the ultimate axial uplift capacity of piles subjected to static compressive loads are available. However, data on ultimate oblique resistance of piles subjected to static compressive loads are limited.

The comparison presented here is classified in three categories:

1. Comparison of present experimental results with results of present semi empirical approach
2. Comparison of results of suggested semi empirical approach with other experimental data from the past investigators
3. Comparison of present experimental results with other experimental data from the past investigators

6.2 Comparison of present experimental results with proposed semi-empirical approach

In the present study, experimental results are compared with suggested semi empirical results. The comparison is presented below.

a) Net axial uplift capacity

Here the experimentally determined net axial uplift capacity values are compared with predicted values of net axial uplift capacity (Explained in Section 5.2.2) shown in Figure 6.1. From Figure 6.1, it is observed that for all % of compressive

loading cases there is a good correlation between the experimental and predicted values of net axial uplift capacity of piles. The predicted values are about 6 to 17% higher than the observed values for L/d=20. However it is 5-21% for L/d=30.

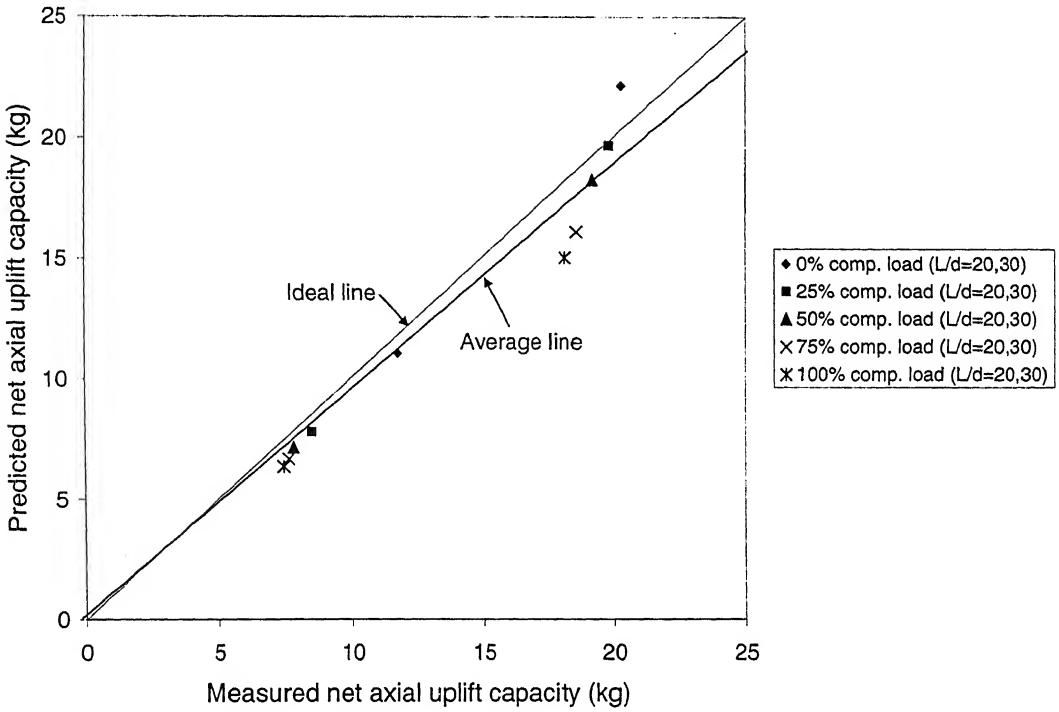

Figure 6.1 Measured vs predicted net uplift capacities of piles

b) Ultimate lateral resistance

The experimentally determined ultimate lateral resistance values are compared with the predicted values. From Figure 6.2 it is observed that the measured and predicted vales are in good agreement. The predicted values are about 24-45% higher than the observed values for L/d=20. However it is 5-25% for L/d=30.

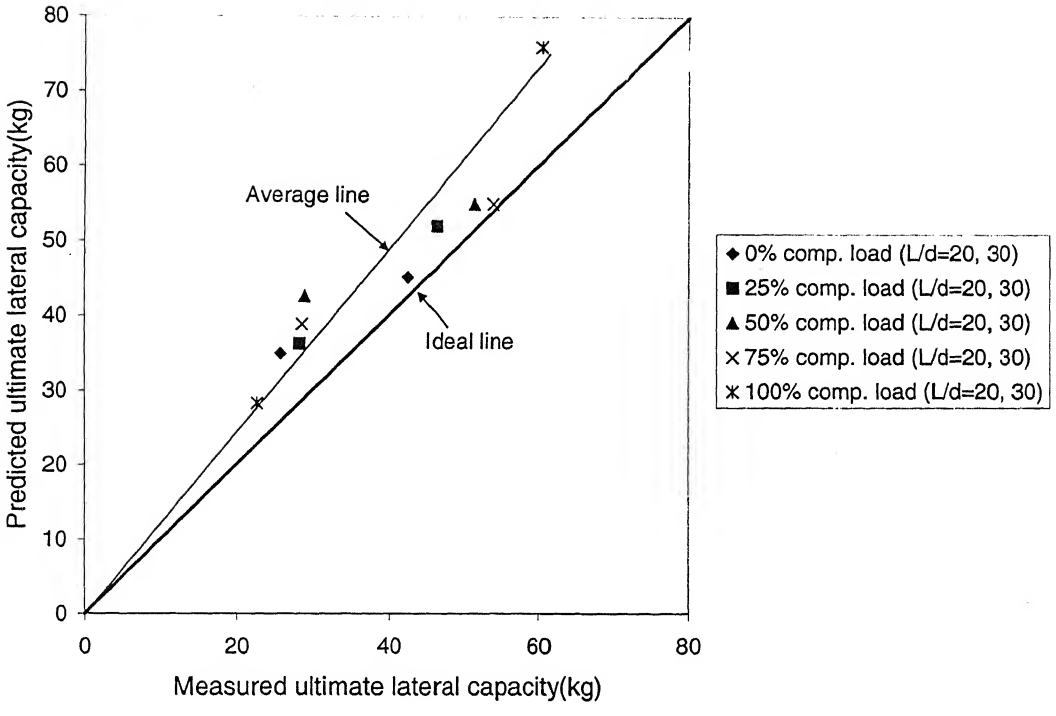

Figure 6.2 Measured vs predicted ultimate lateral capacity of piles

c) Ultimate resistance of piles under oblique pull

Ultimate resistance P_α, under oblique pull subjected to static compressive loads have been plotted against inclination of pile axis α, using polar diagrams, to give a comprehensive view of the effect of inclination. The values of P_α / P_U for different values of α are plotted for P_U / P_L<1 is shown in Figure 6.3 and 6.4. From Figure 6.3 and 6.4 it is seen that for L/d ratio 20 and 30, having P_U / P_L<1, the maximum resistance to oblique pull is mobilized when the inclination of pull is 90^0.

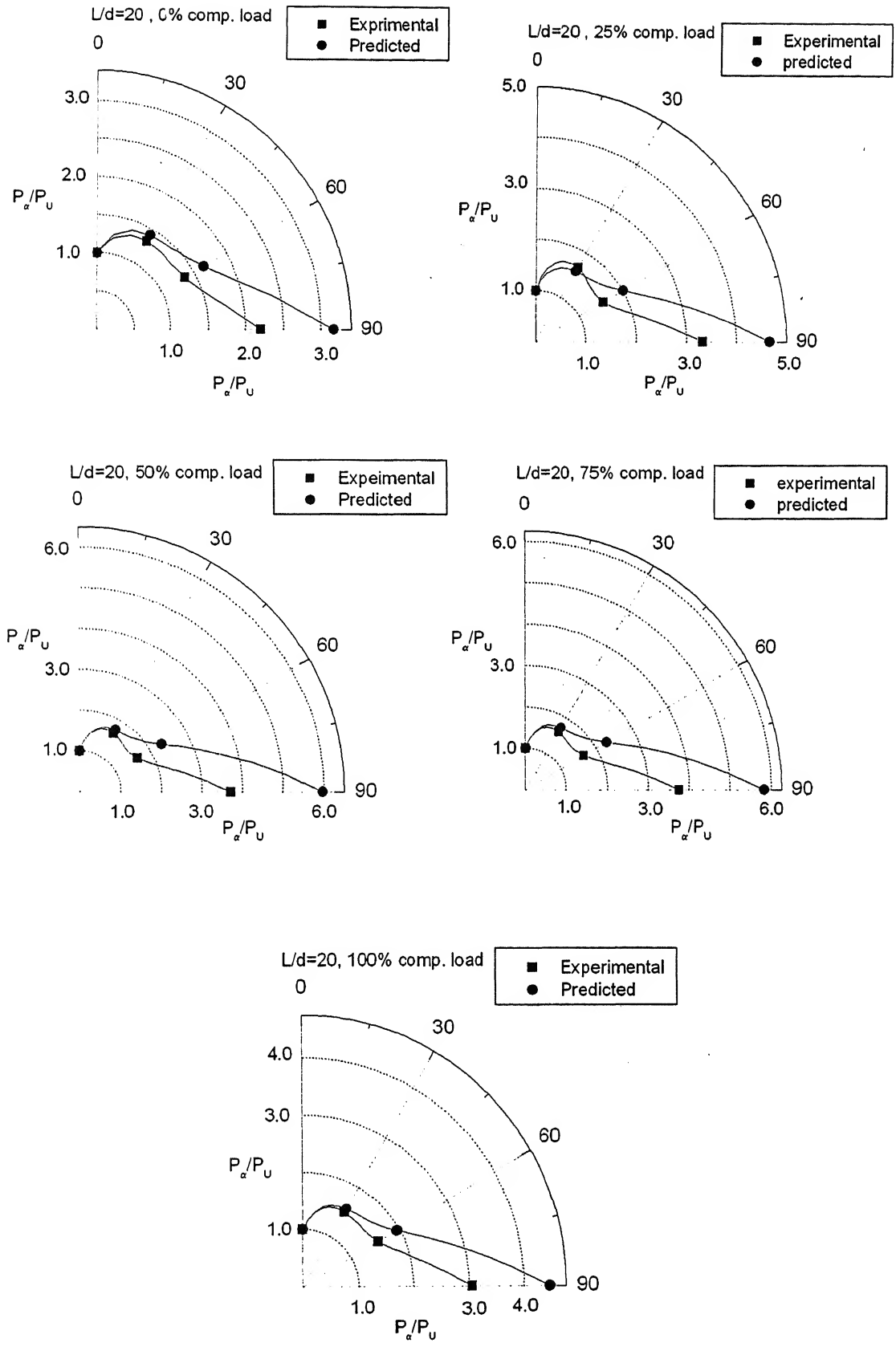

Figure 6.3 Estimated vs observed values of P_α/P_U (L/d=20)

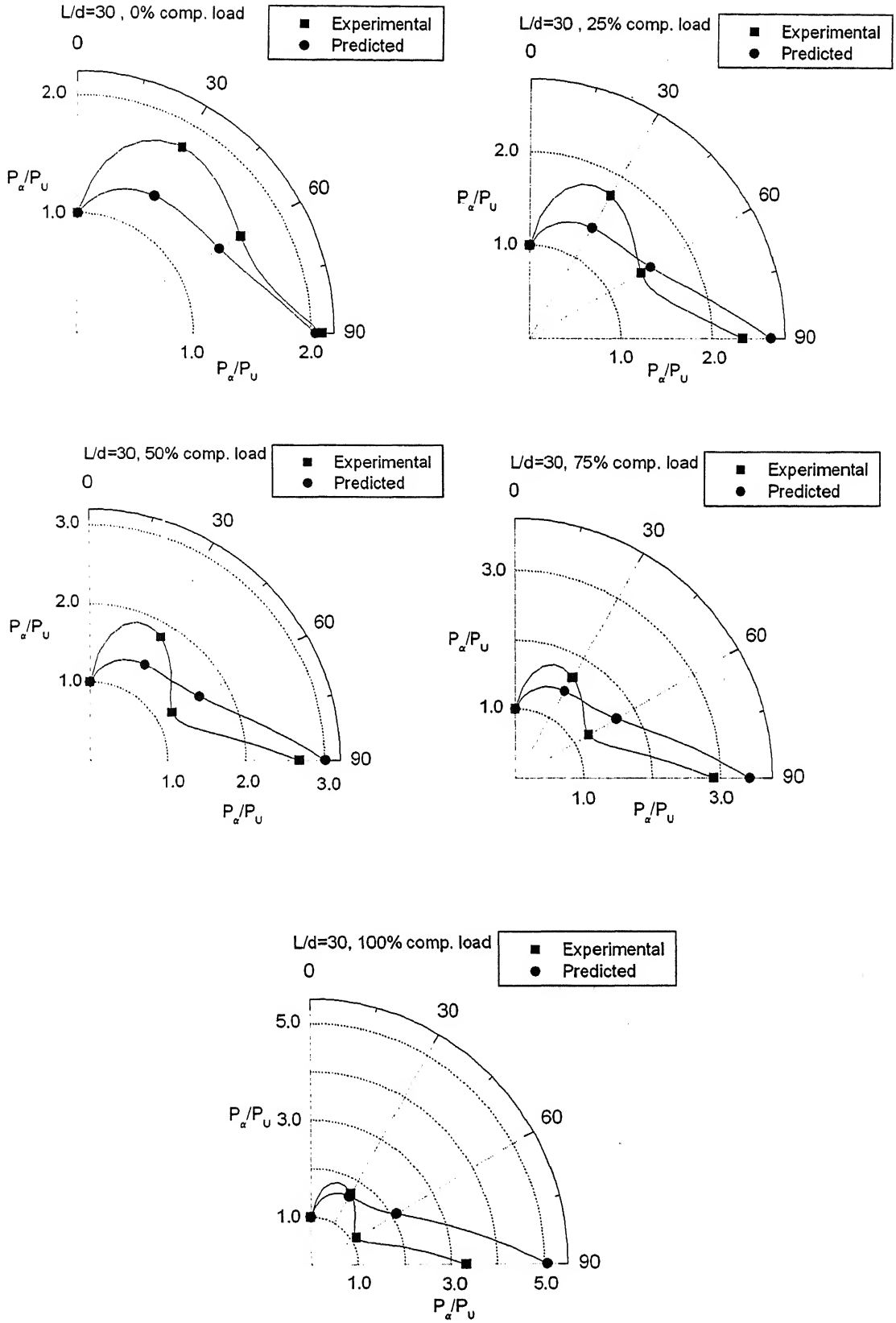

Figure 6.4 Estimated vs observed values of P_α/P_U (L/d=30)

6.3 Comparison of present semi-empirical approach with others experimental data from the past investigators

Present experimental results are compared with past experimental data for different parameters concerned in the study. Data available from the past investigations is limited to oblique pull-out of single piles and uplift cum compressive load case to single piles only. So no comparison is feasible with the past records of data for piles under combined effect of uplift and compressive loads subjected to oblique loads. Comparison is made separately for the different parameters that are involved in the study, i.e. net oblique pull out capacity of piles(Das, selley and Raghu (1976) and Ismael(1989)), decrease in net uplift capacity with stage loading (Dash and Pise(2003))

6. 3.1 Model test results of Das, Seeley and Raghu (1976)

Investigated model test results for the resistance of rigid rough vertical piles subjected to oblique uplift load in loose sand. Wooden piles of diameter 25mm were used as model piles. The embedment lengths to diameter ratios were 12 and 8. The angle of friction, ϕ, at the average density of the test was 31^0. Dry silica sand was used as a foundation medium with an average density of 1510kg/m^3.

The reported gross uplift capacity of piles were 1.3056kg and 2.611kg for L/d=8 and L/d=12 respectively. The predicted gross uplift capacities are 1.328kg and 2.608kg for L/d=8 and L/d=12 respectively. The predicted values are in reasonable agreement with the reported values. The reported ultimate lateral resistance of piles were 2.348kg for L/d=8 and 5.81kg for L/d=12. However the predicted values are taken same as the reported values because the load-displacement diagram for $\alpha=90^0$ condition is not given in paper Das et al (1976).

Theoretical value of ultimate resistance, P_α, of vertical pile under pulling load at inclination α is found out from Equation 5.4. The experimental results along with the predicted values under oblique pulling loads are plotted in dimensionless term P_α/P_u against inclination of pull α in Figure 6.5. Reasonable agreement is observed between the predicted and observed values. For all cases the ultimate resistance to oblique pull is mobilized when the angle of inclination is 90^0 with vertical.

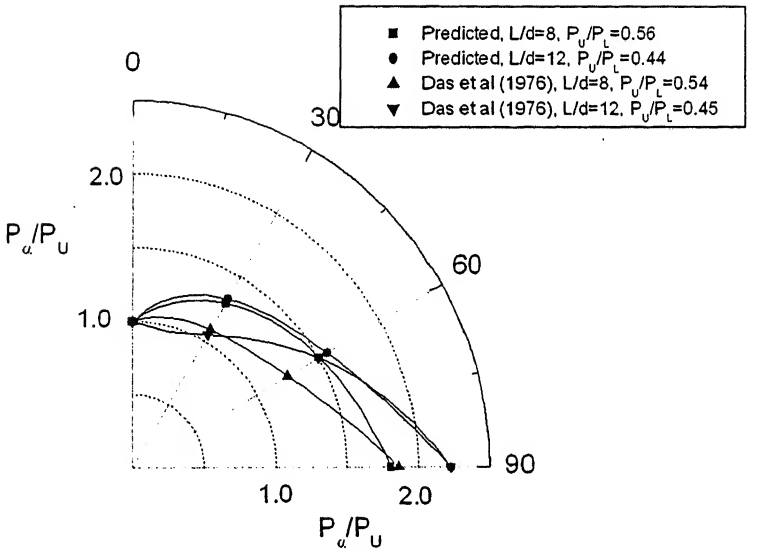

Figure 6.5 Predicted vs observed values of P_α/P_U (Das et al (1976))

6.3.2 Field test results of Ismael (1989)

Ismael (1989) reported field test results on single bored pile under oblique pull. Test included axial uplift test, lateral load test and oblique load test at an angle 30^0 with the pile axis. The piles were bored piles of 101mm diameter, 1.5m long, L/d=14.76. The foundation medium was compact to dense calcareous grey fine to course sand having γ_{sat}= 1766 kg/m^3. The average standard penetration test values were 25. From the N-value, ϕ is assumed to be 37^0 and $\delta = 33.3^0$ (Potyondy, 1961). The net uplift capacity and ultimate lateral capacity of the single pile are determined from Section 5.2.3 and 5.3. The η_h value is assumed as 0.6 kg/cm^3 and the corresponding value of K_{rs} for the bored pile is 2.5x 10^{-3}.

The reported gross uplift capacity and ultimate lateral capacity of bored pile were 22.6 kN and 8.8 kN. The predicted gross uplift capacity and lateral capacity are 15.759kN and 12.75kN. The predicted values are in reasonable agreement with the reported values.

Theoretical value of ultimate resistance, Pα, of vertical pile under pulling load at inclination α is found out from Equation 5.4. The experimental results along with the predicted values under oblique pulling loads are plotted in dimensionless term P_α/P_u against inclination of pull α in Figure 6.6. Reasonable agreement is observed between

the predicted and observed values. By the proposed method the ultimate resistance to oblique pull is mobilized when the inclination of pull is 30^0.

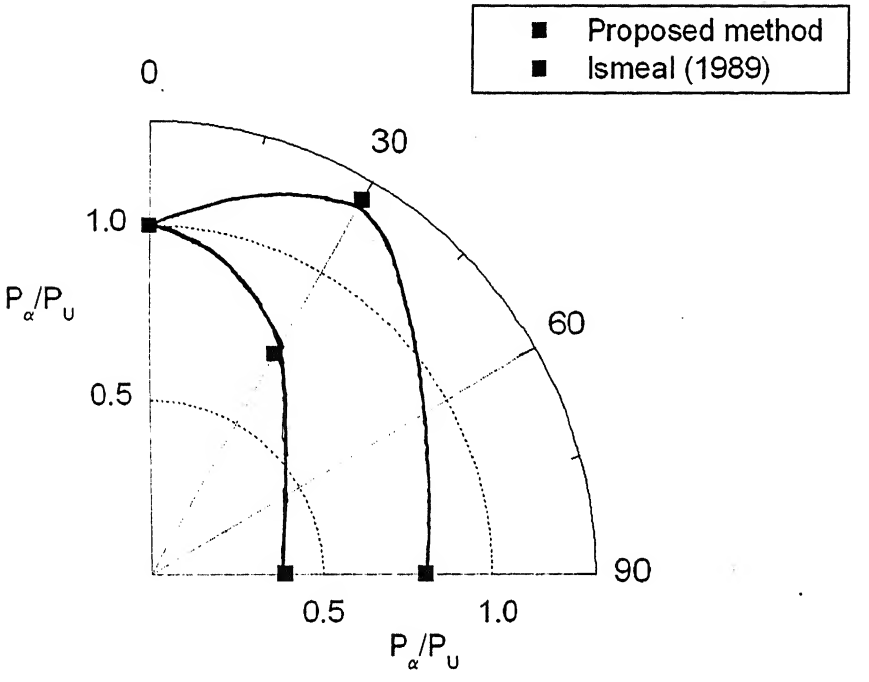

Figure 6.6 Estimated vs observed values of P_α/P_U (Ismael, 1989)

6.3.3 Model Test Results of Dash and Pise (2003)

Dash and Pise (2003) conducted laboratory tests on model tubular steel piles. The model piles were of 25mm outside diameter, 2mm wall thickness and embedment length /diameter ratio's of 8, 16 and 24. The piles were embedded in sand having soil-pile friction angles were 21 and 29 in loose and dense conditions of sand. The piles were subjected to static compressive loads of 0, 25, 50, 75 and 100% of their ultimate capacity in compression and subjected to pull out tests.

The experimental results of Dash and Pise (2003) have been analyzed by semi-empirical approach as explained in Section 5.2. The values of net axial uplift capacity under different % of compressive loading conditions as obtained from semi-empirical approach are compared with the experimental results (shown in Figure 6.7 and 6.8). From Figure 6.7-6.8 it is observed that the predicted values which are off by -54%, -61% and -63% for L/d = 8, 16, and 24 respectively from the experimental values for

loose sand condition however it is of +51%, +54% and +34% for dense sand condition. Reasonable agreement is observed between the predicted and observed values.

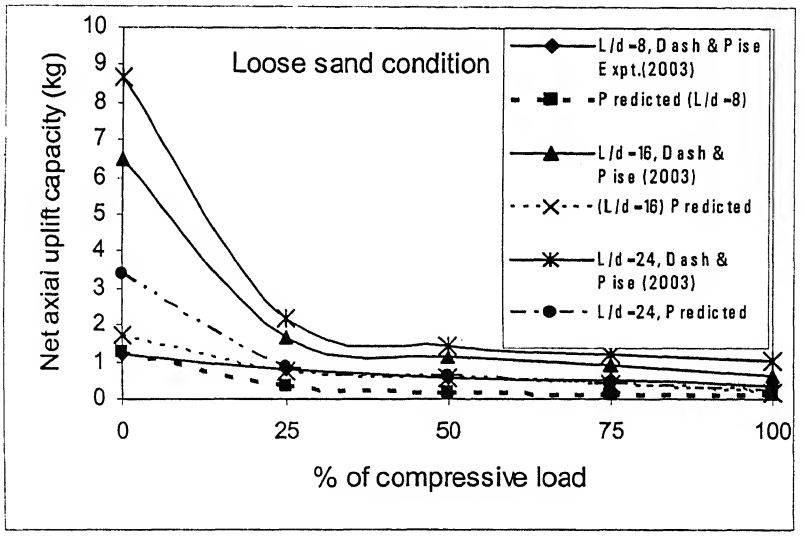

Figure 6.7 Comparison of predicted results with experimental results (Loose sand condition)

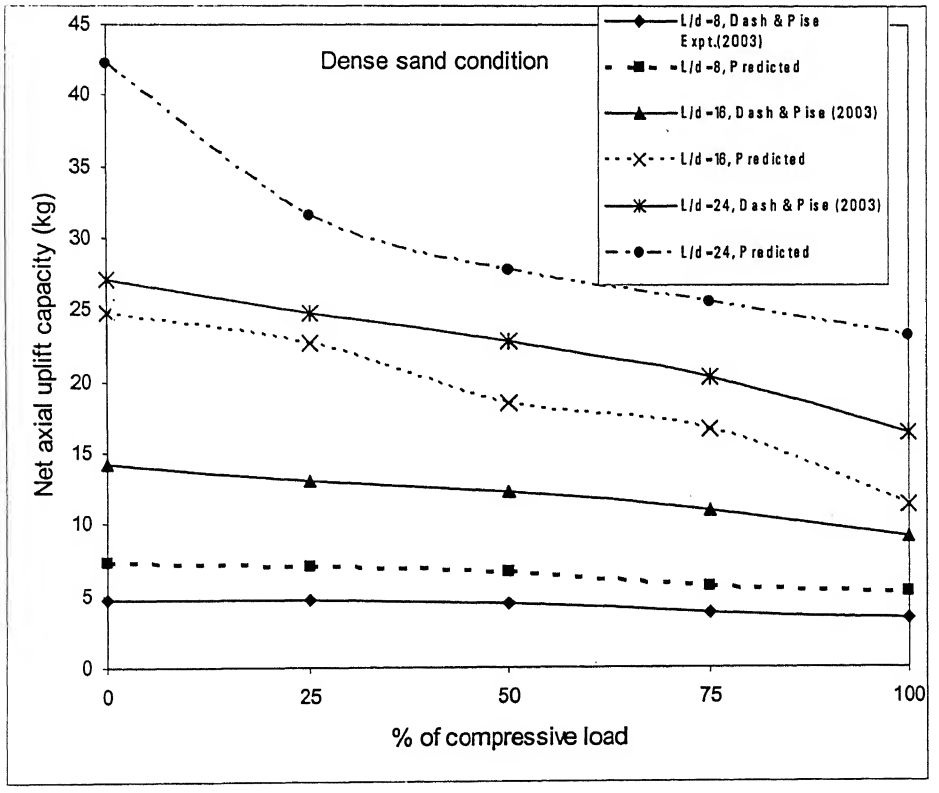

Figure 6.8 Comparison of predicted results with Experimental results (Dense sand condition)

6.4 Comparison of present experimental results with others experimental data from the past investigators

Present experimental results are compared with the past experimental data for different parameters concerned in this study. Data available from the past investigations is limited to pure axial uplift of single piles subjected to static compressive loads (Dash and Pise (2003)). So no comparison is feasible with the past records of the data for oblique pullout capacity of piles subjected to static compressive loads. Some of the researchers (Das, seeley and Raghu(1976), Chattopadhyay and Pise(1986)) produced some results on piles subjected to oblique pulling loads, have been compared with the present experimental data.

6.4.1 Model test results of Dash and Pise (2003)

Dash and Pise (2003) conducted laboratory tests on model tubular steel piles. The model piles were of 25mm outside diameter, 2mm wall thickness and embedment length /diameter ratio's of 8, 16 and 24. The piles were embedded in sand having soil-pile friction angles were 21 and 29 in loose and dense conditions of sand. The piles were subjected to static compressive loads of 0, 25, 50, 75 and 100% of their ultimate capacity in compression and subjected to pull out tests.

Here the net axial uplift capacity of single piles subjected to static compressive loads is compared with the experimental results of Dash and Pise (2003) shown in Figure 6.9. The variation is similar at all conditions. It is observed that the net axial uplift capacity decreases with the increase in % of static compressive loading. Also, for a given static loading condition the net axial uplift capacity increases with the increase in L/d ratio as well as with the soil density. The present experimental net axial uplift capacity values for different static loads in medium dense sand for L/d=20 lies in between the net axial uplift capacity values given by the above authors for piles with L/d=16 and L/d=24 in loose and dense sand conditions. Whereas for L/d=30 in medium dense sand, the values are lying in between the values of L/d=16 and L/d=24 for dense condition of the authors.

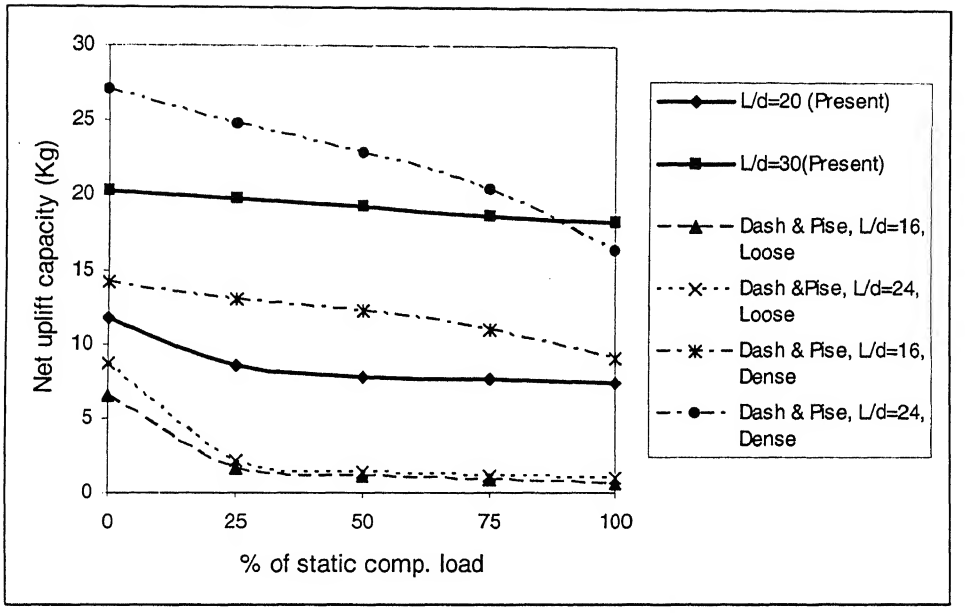

Figure 6.9 Comparison with Dash and Pise (2003)

6.4.2 Model test results of Das, Seeley and Raghu (1976)

Investigated model test results for the resistance of rigid rough vertical piles subjected to oblique uplift load in loose sand. Wooden piles of diameter 25mm were used as model piles. The embedment lengths to diameter ratios were 12 and 8. The angle of friction, ϕ, at the average density of the test was 31^0. Dry silica sand was used as a foundation medium with an average density of $1510kg/m^3$.

The experimental results along with the experimental results of Das et al (1976) under oblique pulling loads are plotted in dimensionless term P_α/P_u against inclination of pull α in Figure 6.10. Reasonable agreement is observed between the two observed results. From Figure 6.10 it is seen that for all values of P_U / P_L<1, the maximum resistance to oblique pull is mobilized when the inclination of pull is 90^0.

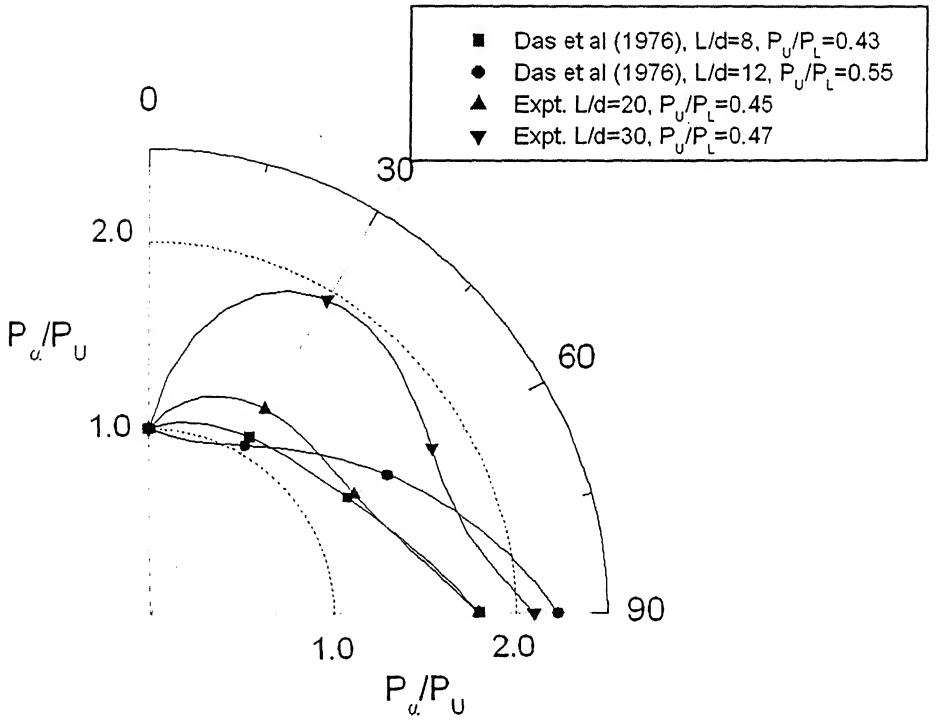

Figure 6.10 Comparison with Das et al (1976) experimental values

6.4.3 Model Test results of Chattopadhyay and Pise (1986)

Chattopadhyay and Pise (1986) reported model tests results on smooth and rough aluminium alloy tubes having 19mm and 21.4mm outside diameters respectively, having embedment lengths 246mm, 496mm and 744mm were embedded in dry Ennore sand of unit weight 1.606 g/cc and angle of shearing resistance of 41^0. The angle of friction between smooth, medium and rough pile and sand were 15^0, 34^0, and 37^0 respectively. The piles fully embedded in sand were tested in vertical position under oblique pull for $\alpha = 0^0, 30^0, 60^0$ and 90^0.

The experimental values of oblique resistance of piles subjected to 0% compressive load is compared with the experimental values of Chattopadhyay and Pise is shown in Figure 6.8. From Figure 6.11 it is seen that reasonable agreement is observed between the two observed results.

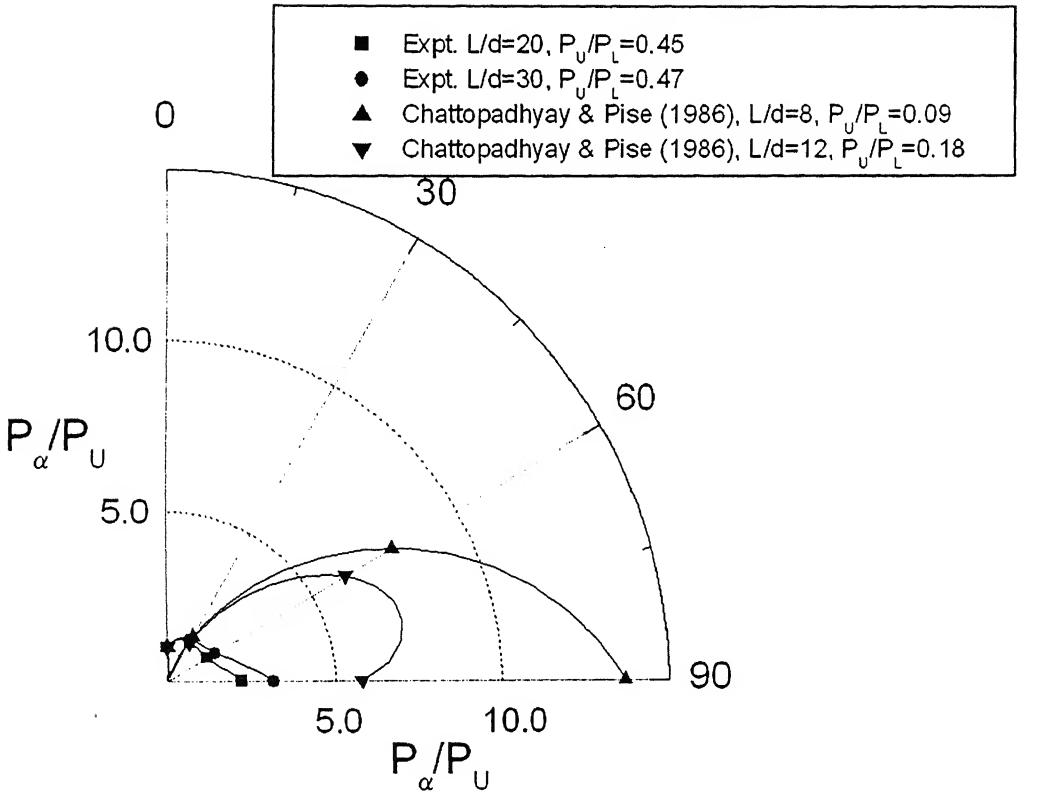

Figure 6.11 Comparison with Chattopadhyay and Pise (1986) experimental values

Chapter VII

Conclusions

A program of model tests was carried out on single steel piles in sand to examine the effect of compressive load on pull-out capacity under oblique loads. Tests included an uplift tests, lateral load tests and oblique tests at an angle of 30^0, 60^0 with the vertical. From the foregoing investigation, following conclusions are drawn

1. Generally the load-displacement responses (i. e. both oblique pull vs axial displacements and oblique pull vs lateral displacements) of the piles subjected to compressive loads under oblique pulling loads are nonlinear.
2. It is observed that if the inclination of the pull with vertical is $\leq 30^0$, the failure of the pile is axial failure and if it is $\geq 60^0$ the failure is due to bending.
3. From the load-displacement responses, it is observed that the axial displacement depends on the normal component of the pull and also the normal displacement depends up on the axial component of the pull.
4. The oblique capacity of piles decreases with increase in % of compressive load.
5. The optimum resistance of piles under compressive load was observed at an angle of inclination 90^0 with vertical.
6. Three semi empirical methods have been proposed to predict the net axial uplift capacity, ultimate lateral capacity and oblique pullout resistance of piles subjected to static compressive loads. The predicted values showed the similar trend.
7. The net axial uplift capacity of single piles subjected to static compressive loads is compared with the experimental results of Dash and Pise (2003). It is observed that in loose condition the estimated values are lesser than the experimental values. However for dense sand condition the estimated values are higher than the experimental values.
8. The test results on model piles by Das, Seeley and Raghu (1976) Chattopadhyay and Pise (1986) and Ismael (1989) and have also been compared with the predictions from the present analysis in oblique condition for 0% compressive loading case. The predicted values show the similar trend.

Scope for future investigations

Experimental investigation on model piles varying parameters like embedment length, roughness of the pile surface, type of pile material, angle of internal friction and cohesion of soil medium with other physical parameters in wide range may be carried out, correlating the results with the field observations.

The present experimental investigation on model single piles can be similarly extended to pile groups also.

The critical angle at transition wherein the failure mode changes from axial to bending is to be predicted by taking various angles of inclinations.

References

1. Adams, J. I. (1975). "Investigation and analysis of transmission tower foundation." *Ontario Hydro Research Division*, Report No. 75-51-H, Toranto, Canada.
2. Adams, J. I. and Hayes, D. C. (1967). "The uplift capacity of shallow foundations." *Ontario Hydro Research Quarterly*, 19(1), 1-33.
3. Alawayn, A. S. Malkawi, A. I. H. and Al-Deeky, H. (1999). "Tension tests on smooth and rough model piles in dry sand." *Can.Geotech. J.*, 36, 746-753.
4. Award, A. and Ayoub, A. (1976). "Ultimate uplift capacity of vertical and inclined piles in cohessionless soil." *Proc., 5th Conf. on Soil Mech, and Found. Engrg.*, Budapest, Hungary, 221-227.
5. Broms, B. (1964). "Lateral resistance of piles in cohesionless soils." *J. Soil Mech. and Found. Engrg.*, ASCE, 90(3), 123-156.
6. Broms, B. (1965). "Discussion to paper by Y. Yoshimi." *J. Soil Mech. and Found. Engrg.*, ASCE, 91(4), 199-205.
7. Chaudhuri, K. P. R. and Symons, M. V. (1983). "Uplift resistance of model single piles." *Proc. Conf. Geotech. Practice in Offshore Engrg.*, Sponsored by Geotech. Engrg. Div., ASCE, Austin, Tex, 335-355.
8. Chattopadyay, B. C. and Pise, P. J. (1986a). "Uplift Capacity of piles in sand." *J. Geotech. Engrg. Div.*, ASCE, 112(9), 888-903.
9. Chattopadyay, B. C. and Pise, P. J. (1986b). "Ultimate resistance of vertical piles to oblique pulling loads." *Proc. Ist East Asian Conf. on Struct. Engrg. and Const.*, Bangkok, 1, 1632-1641.
10. Das, B.M and Seeley, G.R (1975): "Uplift Capacity of Model buried Piles in sand", *J. Geotech. Engrg. Div.*, ASCE, 101(10), 1091-1094.
11. Das, B. M. Seeley, G. R. and Raghu, D. (1976). "Uplift capacity of model piles under oblique loads." *J. Geotech. Engrg. Div.*, ASCE, 12(9), 1009-1013.
12. Das, B. M., Seeley, G. R. and Pfeifle, T. W. (1977). "Pull out resistance of rough piles in granular soils." *Soils and Found.*, 17(3), 72-77.
13. Dash, B. K. and Pise, P. J. (2003). "Effect of compressive load on uplift capacity of model piles." *J. Geotech. Geoenvi. Engrg. Div.*, ASCE, 129(11), 987-992.

14. Downs, D. I. and Chieurzzi, R. (1966). "Transmission tower foundations." *J. Power Div.*, ASCE,92(2), 91-114.

15. Ismael, N. F. and Klym, T. W. (1979) "Uplift and bearing capacity short piers in sand." *J. Geotech. Engrg. Div.*, ASCE, 105(5), 579-594.

16. Ismael, N. F. and Al-sanad, H. A. (1986). "Uplift capacity of bored piles in calacarious soils." *J. Geotech. Engrg. Div.*, ASCE, 112(10), 928-939.

17. Ismael, N. F. (1989). "Field test on bored piles subjected to axial and oblique pull." *J. Geotech. Engrg. Div.,* ASCE, 115(11), 1588-1598.

18. Kraft, L. M. (1991). "Performance of axially loaded pipe piles in sand." *J. Geotech. Engrg.,* 117(2), 272-296.

19. Kulhawy, F. H. (1985). "Drained uplift capacity of drilled shafts." *11th Int. Conf. Soil Mech. Found. Engrg.*, San Francisco, 3, 1549-1551.

20. Kulhemayer, R. L. (1979). "Static and dynamic laterally loaded floating piles." *J. Geotech. Engrg Div.*, ASCE, 105(2), 289-304.

21. Levacher, D. R. and Sieffert, J. G. (1984). "Tests on model tension piles." *J. Geotech. Engrg. Div.*, ASCE, 105(5), 579-593.

22. Liu, Q. F. and Meyerhof, G. G. (1987). "New methods of non-linear analysis of laterally loaded flexible piles." *Comp. and Geomech.*, 3, 151-169.

23. Mayerhof, G. G. and Adams,J. I. (1968). "The ultimate uplift capacity foundations." *Can. Geotech. J.*, 5(4), 225-244.

24. Meyerhof, G. G. and Ranjan, G. (1972). "The bearing capacity of rigid piles under inclined loads in sand-I-vertical piles." *Can. Geotech. J.*, 9, 430-446.

25. Meyerhof, G. G. (1973). "Uplift capacity of foundations under oblique loads." *Can. Geotech. J.*, 10, 64-70.

26. Meyerhof, G. G. and Ranjan, G. (1973). "The bearing capacity of rigid piles under inclined loads in sand-III: pile groups." *Can. Geotech. J.*, 10, 428-438.

27. O'Neill, M. W., Hawkins, R. A. and Mahar, L. J. (1982). "Load transfer mechanism in piles and pile groups." J. *Geotech. Engrg. Div.,* ASCE, 108(12), 1605-1623.

28. Potyondy, J. G. (1971). "Skin friction between various soils and construction materials." *Geotechnique*, London, 11(4), 339-353.

29. Poulos, H.G and Davis, E.H (1980): Pile Foundation Analysis and Design, *John Wiley & Sons*, New York, Ist Ed.

30. Poorooshasb, H. B. and Parameswaran, V. R. (1982). "Uplift of rigid piles in frozen sand", *Soils and Found.*, 22(2), 82-88.

31. Prasad, V. S. N. Y. and Chari, T. R. (1999). "Lateral capacity of model rigid piles in cohessionless soils." *Soils and Found.,* 39(2), 21-29.

32. Patra, N. R. (2001). "Ultimate resistance of piles and pile groups in sand under oblique pulling loads." Ph. D. Thesis, IIT, Kharagpur, India.

33. Pise, P.J (2004): "Pile Foundations under Uplift Loads an Overview", *Indian Geotech. J.*, 34(1), 1-63.

34. Ramanathan, T. S. and Aiyer, P. G. (1970). "Pullout resistance of piles in sand." *J. Int. Society Soil Mech. Found. Engrg.*, 9(2), 189-202.

35. Randolph, M. F. (1981). "The response of flexible piles to lateral loading." *Geotechnique,* 31(2), 247-259.

36. Rowe, R. K. and Poulos, H. G. (1979). "A method for predicting the effect of piles on slope behaviour, *Proc. 3rd Int. Conf. Numerical Methods in Geomechanics*, 3, 1073-1085.

37. Sowa, V.A. (1970) "Pulling Capacity of Concrete Cast in situ Bored Piles", *Can. Geotech. J.*, 7, 482-493.

38. Subba Rao, K. S. and Venkatesh, K. H. (1985). "Uplift behavior of short piles in sand." *Soils and Found.*, 25(2), 01-07.

39. Turner, J. P. and Kulhawy, F. H. (1990). "Drained uplift capacity of drilled shafts under repeated loading." *J. Geotech. Engrg. Div.*, ASCE, 116(3), 470-491.

40. Vesic, A. S. (1970) "Tests on instrumented piles, Ogeechee river state", *J. Geotech. Engrg. Div.*, ASCE, 96(2), 561-584.

41. Yoshimi, Y. (1964). "Piles in cohesionless soil subjected to oblique pull." *J. Geotech. Engrg. Div.*, ASCE, 90(6), 11-24.